Spectroscopic Identification of a Novel Catalytic Reaction of Atomic Hydrogen and the Hydride Ion Product

Randell L. Mills
BlackLight Power, Inc.
493 Old Trenton Road
Cranbury, NJ 08512

From a solution of a Schrödinger-type wave equation with a nonradiative boundary condition based on Maxwell's equations, Mills predicts that atomic hydrogen may undergo a catalytic reaction with certain atomized elements such as cesium and strontium atoms or certain gaseous ions such as Ar^+ which singly or multiply ionize at integer multiples of the potential energy of atomic hydrogen, $27.2\,eV$. The reaction involves a nonradiative energy transfer to form a hydrogen atom that is lower in energy than unreacted atomic hydrogen with the release of energy. Intense extreme ultraviolet (EUV) emission was observed from incandescently heated atomic hydrogen and the atomized catalysts that generated the plasma at low temperatures (e.g. $\approx 10^3\,K$). No emission was observed with cesium, strontium, argon, hydrogen, or an argon-hydrogen mixture (97/3%) alone or when sodium, magnesium, or barium replaced strontium or cesium with hydrogen or with an argon-hydrogen mixture. The emission intensity of the plasma generated by the cesium or strontium catalyst increased significantly with the introduction of argon gas only when Ar^+ emission was observed. Ar^+ which served as a second catalyst was generated by the formation of a plasma with cesium or strontium catalyst. Emission was observed from a continuum state of Cs^{2+} and Ar^{2+} at $53.3\,nm$ and $45.6\,nm$, respectively. The single emission feature with the absence of the other corresponding Rydberg series of lines from these species confirmed the resonate nonradiative energy transfer of $27.2\,eV$ from atomic hydrogen to atomic cesium or Ar^+. The catalysis product, a lower-energy hydrogen atom, was predicted to be a highly reactive intermediate which further reacts to form a novel hydride ion. The predicted hydride ion of hydrogen catalysis by either cesium atom or Ar^+ catalyst is the hydride ion $H^-(1/2)$. This ion was observed spectroscopically at $407\,nm$ corresponding to its predicted binding energy of $3.05\,eV$.

I. INTRODUCTION

A. Novel Hydrogen Chemistry

Based on the solution of a Schrödinger-type wave equation with a nonradiative boundary condition based on Maxwell's equations, Mills [1-31] predicts that atomic hydrogen may undergo a catalytic reaction with certain atomized elements or certain gaseous ions which singly or multiply ionize at integer multiples of the potential energy of atomic hydrogen, $27.2\,eV$. For example, cesium atoms ionize at an integer multiple of the potential energy of atomic hydrogen, $m \cdot 27.2\,eV$. The enthalpy of ionization of Cs to Cs^{2+} has a net enthalpy of reaction of $27.05135\,eV$, which is equivalent to $m=1$ [32]. And, the reaction Ar^{+} to Ar^{2+} has a net enthalpy of reaction of $27.63\,eV$, which is equivalent to $m=1$ [32]. In each case, the reaction involves a nonradiative energy transfer to form a hydrogen atom that is lower in energy than unreacted atomic hydrogen. The product hydrogen atom has an energy state that corresponds to a fractional principal quantum number. Recent analysis of mobility and spectroscopy data of individual electrons in liquid helium show direct experimental confirmation that electrons may have fractional principal quantum energy levels [33]. The lower-energy hydrogen atom is a highly reactive intermediate which further reacts to form a novel hydride ion. We report single line emission from the excited catalyst ion formed by nonradiatively accepting the energy of $27.2\,eV$ from atomic hydrogen. Furthermore, the emission from the predicted hydride ion product was observed spectroscopically. The catalytic reaction with the formation of the hydride ions produces an intense hydrogen plasma which was observed by EUV and visible emission.

Typically the emission of extreme ultraviolet light from hydrogen gas is achieved via a discharge at high voltage, a high power inductively coupled plasma, or a plasma created and heated to extreme temperatures by RF coupling (e.g. $>10^{6}\,K$) with confinement provided by a toroidal magnetic field. Observation of intense extreme ultraviolet (EUV) emission at low temperatures (e.g. $\approx 10^{3}\,K$) from atomic hydrogen and certain atomized elements or certain gaseous ions [2-16] has been reported previously. The only pure elements that were observed to emit

EUV were those wherein the ionization of t electrons from an atom to a continuum energy level is such that the sum of the ionization energies of the t electrons is approximately $m \cdot 27.2\,eV$ where t and m are each an integer. Potassium, cesium, and strontium atoms and Rb^+ ion ionize at integer multiples of the potential energy of atomic hydrogen and caused emission. Whereas, the chemically similar atoms, sodium, magnesium and barium, do not ionize at integer multiples of the potential energy of atomic hydrogen and caused no emission.

Prior studies that support the possibility of a novel reaction of atomic hydrogen which produces an anomalous discharge and produces novel hydride compounds include extreme ultraviolet (EUV) spectroscopy [3-6, 8-16], plasma formation [2-16], power generation [2-4, 9, 31], and analysis of chemical compounds [12, 14-31].

1.) Lines observed at the Institut Fur Niedertemperatur-Plasmaphysik e.V. by EUV spectroscopy could be assigned to transitions of atomic hydrogen to lower energy levels corresponding to lower energy hydrogen atoms and the emission from the excitation of the corresponding hydride ions [6]. For example, the product of the catalysis of atomic hydrogen with potassium metal, $H\left[\frac{a_H}{4}\right]$ may serve as both a catalyst and a reactant to form $H\left[\frac{a_H}{3}\right]$ and $H\left[\frac{a_H}{6}\right]$. The transition of $H\left[\frac{a_H}{4}\right]$ to $H\left[\frac{a_H}{6}\right]$ induced by a multipole resonance transfer of $54.4\,eV$ $(2 \cdot 27.2\,eV)$ and a transfer of $40.8\,eV$ with a resonance state of $H\left[\frac{a_H}{3}\right]$ excited in $H\left[\frac{a_H}{4}\right]$ is represented by

$$H\left[\frac{a_H}{4}\right] + H\left[\frac{a_H}{4}\right] \rightarrow H\left[\frac{a_H}{6}\right] + H\left[\frac{a_H}{3}\right] + 176.8\,eV \qquad (1)$$

The predicted $176.8\,eV$ (70.2 Å) photon is a close match with the observed 73.0 Å line. The energy of this line emission corresponds to an equivalent temperature of 1,000,000 °C and an energy over 100 times the energy of combustion of hydrogen.

2.) Transitions of atomic hydrogen to lower energy levels corresponding to lower energy hydrogen atoms has been identified in the extreme ultraviolet emission spectrum from interstellar medium [34].

3.) Observation of intense extreme ultraviolet (EUV) emission has been reported at low temperatures (e.g. $\approx 10^3\,K$) from atomic hydrogen and certain atomized elements or certain gaseous ions [2-16]. The only pure elements that were observed to emit EUV were those wherein the ionization of t electrons from an atom to a continuum energy level is such that the sum of the ionization energies of the t electrons is approximately $m \cdot 27.2\,eV$ where t and m are each an integer. Potassium, cesium, and strontium atoms and Rb^+ ion ionize at integer multiples of the potential energy of atomic hydrogen and caused emission. Whereas, the chemically similar atoms, sodium, magnesium, and barium do not ionize at integer multiples of the potential energy of atomic hydrogen and caused no emission.

4.) An energetic plasma in hydrogen was generated using strontium atoms as the catalyst. The plasma formed at 1% of the theoretical or prior known voltage requirement with 4,000-7,000 times less power input power compared to noncatalyst controls, sodium, magnesium, or barium atoms, wherein the plasma reaction was controlled with a weak electric field [4, 9]. The light output for power input increased to 8600 times that of the control when argon was added to the hydrogen strontium plasma to form catalyst Ar^+ [3].

5.) The optically measured output power of gas cells for power supplied to the glow discharge increased by over two orders of magnitude depending on the presence of less than 1% partial pressure of certain of catalysts in hydrogen gas or argon-hydrogen gas mixtures [2].

6.) In experiments performed at the Institut Fur Niedertemperatur-Plasmaphysik e.V., an anomalous plasma formed with hydrogen-potassium mixtures wherein the plasma decayed with a two second half-life which was the thermal decay time of the filament which dissociated molecular hydrogen to atomic hydrogen when the electric field was set to zero [7, 10]. This experiment showed that hydrogen line emission was occurring even though the voltage between the heater wires was set to and measured to be zero and indicated that the emission was due to a

reaction of potassium catalyst with atomic hydrogen which confirms a new chemical source of power.

7.) A plasma of hydrogen and certain alkali ions formed at low temperatures (e.g. $\approx 10^3\,K$) as recorded via EUV spectroscopy and the hydrogen Balmer and alkali line emissions in the visible range. The observed plasma formed at low temperatures (e.g. $\approx 10^3\,K$) from atomic hydrogen generated at a tungsten filament that heated a titanium dissociator and a catalyst comprising one of potassium, rubidium, cesium, and their carbonates and nitrates. These atoms and ions ionize to provide a catalyst with a net enthalpy of reaction of an integer multiple of the potential energy of atomic hydrogen ($m \cdot 27.2\,eV$ $m = integer$) to within 0.17 eV and comprise only a single ionization in the case of a potassium or rubidium ion. Whereas, the chemically similar atoms of sodium and sodium and lithium carbonates and nitrates which do not ionize with these constraints caused no emission. To test the electric dependence of the emission, the weak electric field of about 1 V/cm was set and measured to be zero in $< 0.5\,X\,10^{-6}$ sec. An anomalous afterglow duration of about one to two seconds was recorded in the case of potassium, rubidium, cesium, K_2CO_3, $RbNO_3$, and $CsNO_3$. Hydrogen line or alkali line emission was occurring even though the voltage between the heater wires was set to and measured to be zero. These atoms and ions ionize to provide a catalyst with a net enthalpy of reaction of an integer multiple of the potential energy of atomic hydrogen to within less than the thermal energies at $\approx 10^3\,K$ and comprise only a single ionization in the case of a potassium or rubidium ion. Since the thermal decay time of the filament for dissociation of molecular hydrogen to atomic hydrogen was similar to the anomalous plasma afterglow duration, the emission was determined to be due to a reaction of atomic hydrogen with a catalyst that did not require the presence of an electric field to be functional.

8.) Reports of the formation of novel compounds provide substantial evidence supporting a novel reaction of hydrogen as the mechanism of the observed EUV emission and anomalous discharge. Novel hydrogen compounds have been isolated as products of the reaction of atomic hydrogen with atoms and ions identified as catalysts in the reported EUV studies [2-31]. Novel inorganic alkali and alkaline earth hydrides of the formula MH^* and MH^*X wherein M is the metal,

X, is a singly negatively charged anion, and H^* comprises a novel high binding energy hydride ion were synthesized in a high temperature gas cell by reaction of atomic hydrogen with a catalyst such as potassium metal and MH, MX or MX_2 corresponding to an alkali metal or alkaline earth metal compound, respectively [17, 20-21]. Novel hydride compounds were identified by 1.) time of flight secondary ion mass spectroscopy which showed a dominant hydride ion in the negative ion spectrum, 2.) X-ray photoelectron spectroscopy which showed novel hydride peaks and significant shifts of the core levels of the primary elements bound to the novel hydride ions, 3.) ^1H nuclear magnetic resonance spectroscopy (NMR) which showed extraordinary upfield chemical shifts compared to the NMR of the corresponding ordinary hydrides, and 4.) thermal decomposition with analysis by gas chromatography, and mass spectroscopy which identified the compounds as hydrides [17, 20].

An upfield shifted NMR peak is consistent with a hydride ion with a smaller radius as compared with ordinary hydride since a smaller radius increases the shielding or diamagnetism. Thus, the NMR shows that the hydride formed in the catalytic reaction has been reduced in distance to the nucleus indicating that the electrons are in a lower-energy state. Compared to the shift of known corresponding hydrides the NMR provides direct evidence of reduced energy state hydride ions.

The NMR results confirm the identification of novel hydride compounds MH^*X, MH^*, and MH_2^* wherein M is the metal, X, is a halide, and H^* comprises a novel high binding energy hydride ion. For example, large distinct upfield resonances were observed at -4.6 ppm and -2.8 ppm in the case of KH^*Cl and KH^*, respectively. Whereas, the resonances for the ordinary hydride ion of KH were observed at 0.8 and 1.1 ppm. The presence of a halide in each compound MH^*X does not explain the upfield shifted NMR peak since the same NMR spectrum was observed for an equimolar mixture of the pure hydride and the corresponding alkali halide (MH/MX) as was observed for the pure hydride, MH. The synthesis of novel hydrides such as KH^* with upfield shifted peaks prove that the hydride ion is different from the hydride ion of the corresponding known compound of the same composition. The

reproducibility of the syntheses and the results from five independent laboratories confirm the formation of novel hydride ions.

The mechanism of EUV emission and formation of novel hydrides can not be explained by the conventional chemistry of hydrogen, but it is predicted by a solution of the Schrödinger equation with a nonradiative boundary constraint put forward by Mills [1]. Mills predicts that certain atoms or ions serve as catalysts to release energy from hydrogen to produce an increased binding energy hydrogen atom called a *hydrino atom* having a binding energy of

$$Binding\ Energy = \frac{13.6\ eV}{n^2} \tag{2}$$

where

$$n = \frac{1}{2}, \frac{1}{3}, \frac{1}{4}, \ldots, \frac{1}{p} \tag{3}$$

and p is an integer greater than 1, designated as $H\left[\frac{a_H}{p}\right]$ where a_H is the radius of the hydrogen atom. Hydrinos are predicted to form by reacting an ordinary hydrogen atom with a catalyst having a net enthalpy of reaction of about

$$m \cdot 27.2\ eV \tag{4}$$

where m is an integer. This catalysis releases energy from the hydrogen atom with a commensurate decrease in size of the hydrogen atom, $r_n = na_H$. For example, the catalysis of $H(n=1)$ to $H(n=1/2)$ releases $40.8\ eV$, and the hydrogen radius decreases from a_H to $\frac{1}{2}a_H$.

The excited energy states of atomic hydrogen are also given by Eq. (2) except that

$$n = 1, 2, 3, \ldots \tag{5}$$

The $n=1$ state is the "ground" state for "pure" photon transitions (the $n=1$ state can absorb a photon and go to an excited electronic state, but it cannot release a photon and go to a lower-energy electronic state). However, an electron transition from the ground state to a lower-energy state is possible by a nonradiative energy transfer such as multipole coupling or a resonant collision mechanism. These lower-energy states have fractional quantum numbers, $n = \frac{1}{\text{integer}}$. Processes that occur without photons and that require collisions are common. For example,

the exothermic chemical reaction of $H+H$ to form H_2 does not occur with the emission of a photon. Rather, the reaction requires a collision with a third body, M, to remove the bond energy-$H+H+M \rightarrow H_2+M^*$ [35]. The third body distributes the energy from the exothermic reaction, and the end result is the H_2 molecule and an increase in the temperature of the system. Some commercial phosphors are based on nonradiative energy transfer involving multipole coupling. For example, the strong absorption strength of Sb^{3+} ions along with the efficient nonradiative transfer of excitation from Sb^{3+} to Mn^{2+}, are responsible for the strong manganese luminescence from phosphors containing these ions [36]. Similarly, the $n=1$ state of hydrogen and the $n=\frac{1}{\text{integer}}$ states of hydrogen are nonradiative, but a transition between two nonradiative states is possible via a nonradiative energy transfer, say $n=1$ to $n=1/2$. In these cases, during the transition the electron couples to another electron transition, electron transfer reaction, or inelastic scattering reaction which can absorb the exact amount of energy that must be removed from the hydrogen atom. Thus, a catalyst provides a net positive enthalpy of reaction of $m \cdot 27.2\ eV$ (i.e. it absorbs $m \cdot 27.2\ eV$ where m is an integer). Certain atoms or ions serve as catalysts which resonantly accept energy from hydrogen atoms and release the energy to the surroundings to effect electronic transitions to fractional quantum energy levels. Recent analysis of mobility and spectroscopy data of individual electrons in liquid helium show direct experimental evidence that electrons may have fractional principal quantum energy levels [33].

The catalysis of hydrogen involves the nonradiative transfer of energy from atomic hydrogen to a catalyst which may then release the transferred energy by radiative and nonradiative mechanisms. As a consequence of the nonradiative energy transfer, the hydrogen atom becomes unstable and emits further energy until it achieves a lower-energy nonradiative state having a principal energy level given by Eq. (2-3).

The energy released during catalysis may undergo internal conversion and ionize or excite molecular and atomic hydrogen resulting in hydrogen emission which includes well characterized ultraviolet lines such as the Lyman series. Lyman a emission was sought by EUV

spectroscopy. The energy released during catalysis may also undergo internal conversion and cause alkali line emission. The existence of Balmer emission requires that Lyman emission is also generated. This confirms that a hydrogen plasma exists. Lyman a emission was sought by EUV spectroscopy, and Balmer and alkali line emission was sought by visible spectroscopy.

B. Catalysts

The emission observed EUV emission could not be explained by conventional chemistry; rather it must have been due to a novel chemical reaction between catalyst and atomic hydrogen. According to Mills [1], a catalytic system is provided by the ionization of t electrons from an atom or ion to a continuum energy level such that the sum of the ionization energies of the t electrons is approximately $m\,X\,27.2\,eV$ where m is an integer.

Strontium

One such catalytic system involves strontium. The first through the fifth ionization energies of strontium are $5.69484\,eV$, $11.03013\,eV$, $42.89\,eV$, $57\,eV$, and $71.6\,eV$, respectively [32]. The ionization reaction of Sr to Sr^{5+}, $(t=5)$, then, has a net enthalpy of reaction of $188.2\,eV$, which is equivalent to $m=7$ in Eq. (4).

$$188.2\,eV + Sr(m) + H\left[\frac{a_H}{p}\right] \rightarrow Sr^{5+} + 5e^- + H\left[\frac{a_H}{(p+7)}\right] + [(p+7)^2 - p^2]X13.6\,eV \qquad (6)$$

$$Sr^{5+} + 5e^- \rightarrow Sr(m) + 188.2\,eV \qquad (7)$$

And, the overall reaction is

$$H\left[\frac{a_H}{p}\right] \rightarrow H\left[\frac{a_H}{(p+7)}\right] + [(p+7)^2 - p^2]X13.6\,eV \qquad (8)$$

Argon Ion

Argon ions can also provide a net enthalpy of a multiple of that of the potential energy of the hydrogen atom. The second ionization energy of argon is $27.63\,eV$. The reaction Ar^+ to Ar^{2+} has a net enthalpy of reaction of $27.63\,eV$, which is equivalent to $m=1$ in Eq. (4).

$$27.63\,eV + Ar^+ + H\left[\frac{a_H}{p}\right] \rightarrow Ar^{2+} + e^- + H\left[\frac{a_H}{(p+1)}\right] + [(p+1)^2 - p^2]X13.6\,eV \tag{9}$$

$$Ar^{2+} + e^- \rightarrow Ar^+ + 27.63\,eV \tag{10}$$

And, the overall reaction is

$$H\left[\frac{a_H}{p}\right] \rightarrow H\left[\frac{a_H}{(p+1)}\right] + [(p+1)^2 - p^2]X13.6\,eV \tag{11}$$

Cesium

A catalytic system is provided by the ionization of 2 electrons from a cesium atom each to a continuum energy level such that the sum of the ionization energies of the 2 electrons is approximately $27.2\,eV$. The first and second ionization energies of cesium are $3.89390\,eV$ and $23.15745\,eV$, respectively [32]. The double ionization ($t=2$) reaction of Cs to Cs^{2+}, then, has a net enthalpy of reaction of $27.05135\,eV$, which is equivalent to $m=1$ in Eq. (4).

$$27.05135\,eV + Cs(m) + H\left[\frac{a_H}{p}\right] \rightarrow Cs^{2+} + 2e^- + H\left[\frac{a_H}{(p+1)}\right] + [(p+1)^2 - p^2]X13.6\,eV \tag{12}$$

$$Cs^{2+} + 2e^- \rightarrow Cs(m) + 27.05135\,eV \tag{13}$$

And, the overall reaction is

$$H\left[\frac{a_H}{p}\right] \rightarrow H\left[\frac{a_H}{(p+1)}\right] + [(p+1)^2 - p^2]X13.6\,eV \tag{14}$$

C. Hydride Ion

A novel hydride ion having extraordinary chemical properties given by Mills [1] is predicted to form by the reaction of an electron with

a hydrino (Eq. (15)). The resulting hydride ion is referred to as a hydrino hydride ion, designated as $H^-(1/p)$.

$$H\left[\frac{a_H}{p}\right]+e^- \rightarrow H^-(1/p) \tag{15}$$

The hydrino hydride ion is distinguished from an ordinary hydride ion having a binding energy of 0.8 eV. The hydrino hydride ion is predicted [1] to comprise a hydrogen nucleus and two indistinguishable electrons at a binding energy according to the following formula:

$$Binding\ Energy = \frac{\hbar^2\sqrt{s(s+1)}}{8\mu_e a_0^2\left[\frac{1+\sqrt{s(s+1)}}{p}\right]^2} - \frac{\pi\mu_0 e^2\hbar^2}{m_e^2 a_0^3}\left(1+\frac{2^2}{\left[\frac{1+\sqrt{s(s+1)}}{p}\right]^3}\right) \tag{16}$$

where p is an integer greater than one, $s=1/2$, π is pi, $\hbar$ is Planck's constant bar, μ_o is the permeability of vacuum, m_e is the mass of the electron, μ_e is the reduced electron mass, a_o is the Bohr radius, and e is the elementary charge. The ionic radius is

$$r_1 = \frac{a_0}{p}\left(1+\sqrt{s(s+1)}\right);\ s=\frac{1}{2} \tag{17}$$

From Eq. (17), the radius of the hydrino hydride ion $H^-(1/p);\ p=\text{integer}$ is $\frac{1}{p}$ that of ordinary hydride ion, $H^-(1/1)$. Compounds containing hydrino hydride ions have been isolated as products of the reaction of atomic hydrogen with atoms and ions identified as catalysts by EUV emission [2-31].

We report that plasma that emitted intense EUV formed at low temperatures (e.g. $\approx 10^3\ K$) from atomic hydrogen generated at a tungsten filament and atomic strontium or cesium catalyst (Eqs. (6-8) and (12-14), respectively) which were vaporized from the metal by heating. A first catalyst may produce a second catalyst from a source of the second catalyst. For example, a plasma may be formed using atomic hydrogen

and strontium catalyst (Eqs. (6-8)). If argon was added to the plasma, then catalyst Ar^+ (Eqs. (9-11)) would be produced from argon. Second catalyst Ar^+ would in term generate more Ar^+ which may dominate the catalysis reaction. The emission intensity of the plasma generated by the strontium catalyst increased significantly with the introduction of argon gas only when Ar^+ emission was observed. No emission was observed with cesium, strontium, argon, or hydrogen alone or when sodium, magnesium, or barium replaced strontium or cesium with hydrogen or with an argon-hydrogen mixture.

Characteristic emission was observed from a continuum state of Cs^{2+} and Ar^{2+} which confirmed the resonate nonradiative energy transfer of 27.2 eV from atomic hydrogen to atomic cesium or Ar^+, respectively. The predicted $H^-(1/2)$ hydride ion of hydrogen catalysis by either cesium atom or Ar^+ catalyst given by Eqs. (12-14) and Eqs. (9-11), respectively and Eq. (16) was observed spectroscopically at 407 nm corresponding to its predicted binding energy of 3.05 eV.

II. EXPERIMENTAL

A. EUV, UV, and Visible Spectroscopy

Due to the extremely short wavelength of this radiation, "transparent" optics do not exist for EUV spectroscopy. Therefore, a windowless arrangement was used wherein the source was connected to the same vacuum vessel as the grating and detectors of the EUV spectrometer. Windowless EUV spectroscopy was performed with an extreme ultraviolet spectrometer that was mated with the cell. Differential pumping permitted a high pressure in the cell as compared to that in the spectrometer. This was achieved by pumping on the cell outlet and pumping on the grating side of the collimator that served as a pin-hole inlet to the optics. The cell was operated under gas flow conditions while maintaining a constant gas pressure in the cell with a mass flow controller.

The experimental set up shown in Figure 1 comprised a quartz cell which was 500 mm in length and 50 mm in diameter. The cell had three ports for gas inlet, outlet, and photon detection The cell pump was a

mechanical pump. A second gas port from a line common with the cell inlet could supply gas to the cell from the monochromator of the spectrometer according to a special method described below. The spectrometer was continuously evacuated to $10^{-4}-10^{-6}$ torr by a turbomolecular pump with the pressure read by a cold cathode pressure gauge. The EUV spectrometer was connected to the cell light source with a 1.5 mm X 5 mm collimator which provided a light path to the slits of the EUV spectrometer. The collimator also served as a flow constrictor of gas from the cell. Valves were between the cell and the mechanical pump, the cell and the monochromator, the monochromator and the gas supply, and the monochromator and its turbo pump.

A tungsten filament heater and hydrogen dissociator (0.508 mm in diameter and 800 cm in length, total resistance ~2.5 ohm) and, in the case of the control hydrogen gas experiments, a titanium cylindrical screen (300 mm long and 40 mm in diameter) that performed as a second hydrogen dissociator were inside the quartz cell. A new dissociator was used for each control hydrogen gas experiment. The filament was coiled on a grooved ceramic tube support to maintain its shape when heated. The return lead passed through the inside of the ceramic tube. The titanium screen was electrically floated. The power was applied to the filament by a Sorensen 80-13 power supply which was controlled by a constant power controller. The temperature of the tungsten filament was estimated to be in the range of 1100 to 1500 °C. The external cell wall temperature was about 700 °C. Except where indicated, the gas was ultrahigh purity hydrogen, argon-hydrogen mixture (97/3%), or an argon-hydrogen mixture (95/5%). Except where indicated, the gas pressure inside the cell was maintained at about 300 mtorr with a hydrogen flow rate of 5.5 sccm, an argon-hydrogen mixture (97/3%) flow rate of 5.5 sccm, or an argon flow rate of 5.2 sccm and a hydrogen flow rate of 0.3 sccm, respectively. Each gas flow was controlled by a 20 sccm range mass flow controller (MKS 1179A21CS1BB) with a readout (MKS type 246). The entire quartz cell was enclosed inside an insulation package comprised of Zircar AL-30 insulation. Several K type thermocouples were placed in the insulation to measure key temperatures of the cell and insulation. The thermocouples were read with a multichannel computer data acquisition system.

In the present study, the light emission phenomena was studied for 1.) hydrogen, argon, neon, and helium alone; 2.) sodium, magnesium, barium, cesium, and strontium metals alone; 3.) sodium, magnesium, barium, cesium, and strontium with hydrogen; 4.) sodium, magnesium, barium, cesium, and strontium with an argon-hydrogen mixture (97/3%), and 5.) cesium and strontium with argon-hydrogen mixtures. The pure elements of sodium, magnesium, barium, cesium, and strontium were placed in the bottom of the cell and vaporized by filament heating. The power applied to the filament was 300 W in the case of strontium and up to 600 W in the case of magnesium, barium, and sodium metals. The voltage across the filament was about 55 V and the current was about 5.5 A at 300 W. For the controls, magnesium, barium, and sodium metals, the cell was increased in temperature to the maximum permissible with the power supply.

The light emission was introduced to an EUV spectrometer for spectral measurement. The spectrometer was a McPherson 0.2 meter monochromator (Model 302, Seya-Namioka type) equipped with a 1200 lines/mm holographic grating with a platinum coating (except that a MgF_2 coated grating was used for an experiment with a cesium- argon-hydrogen mixture as indicated in the figure caption of Figure 31). This grating has a very low efficiency at the region of hydrogen Lyman α. The wavelength region covered by the monochromator was $30-560\,nm$. A channel electron multiplier (CEM) was used to detect the EUV light. The wavelength resolution was about $1\,nm$ (FWHM) with an entrance and exit slit width of $300\,\mu m$. The vacuum inside the monochromator was maintained below $5\,X\,10^{-4}$ torr by a turbo pump. The EUV spectrum ($40-160\,nm$) of the cell emission with cesium or strontium present was recorded at about the point of the maximum Lyman a emission.

To achieve higher sensitivity at the shorter EUV wavelengths, the light emission was recorded with a McPherson 4° grazing incidence EUV spectrometer (Model 248/310G) equipped with a grating having 600 G/mm with a radius of curvature of $\approx 1\,m$. The angle of incidence was 87°. The wavelength region covered by the monochromator was $1-65\,nm$. The wavelength resolution was about $0.1\,nm$ (FWHM) with an entrance and exit slit width of $50\,\mu m$. A channel electron multiplier (CEM) was

used to detect the EUV light. The vacuum inside the monochromator was maintained below $5X10^{-4}$ torr by a turbo pump.

The EUV/UV/VIS spectrum ($40-560\,nm$) of the cell emission with hydrogen alone was recorded with a photomultiplier tube (PMT) and a sodium salicylate scintillator. The PMT (Model R1527P, Hamamatsu) used has a spectral response in the range of $185-680\,nm$ with a peak efficiency at about $400\,nm$. The scan interval was $0.4\,nm$. The inlet and outlet slit were $500\,\mu m$ with a corresponding wavelength resolution of $2\,nm$.

B. Standard Hydrogen, Argon, and Cesium Emission Spectrum

Standard extreme ultraviolet emission spectra of atomic and molecular hydrogen, argon, and cesium were obtained with a microwave plasma system and an EUV spectrometer. The microwave generator was a Opthos model MPG-4M generator (Frequency: 2450 MHz). The output power was set at about 85 W. Hydrogen or argon was flowed through a quartz tube (1.25 cm ID, 20 cm long) at 500 mtorr. The tube was fitted with an Opthos coaxial microwave cavity (Evenson cavity), and was directly connected to the collimator port of an EUV spectrometer. The EUV spectrometer was a McPherson model 302 (Seya-Namioka type) normal incidence monochromator. The monochromator slits were $100X100\,\mu m$. A sodium salicylate converter was used, and the emission was detected with a photomultiplier tube detector (Hamamatsu R1527P).

In order to record the standard cesium spectrum, a cesium side-arm reservoir was joined to the quartz tube. The reservoir comprised a 1.25 cm ID Pyrex tube with a sealed capillary tip at the end that attached to the microwave plasma quartz tube. In a drybox, about 0.5 g of cesium metal was placed in the reservoir through the other open end of the Pyrex tube. The Pyrex tube was then capped with a septum and was flame-sealed outside the drybox. A glass-capped magnetic bar was placed inside the quartz tube, which was then connected to EUV spectrometer and a gas/vacuum line. After a good vacuum (~10-5 torr) was obtained, the capillary tip on the cesium reservoir was broken through by moving the magnetic bar with an external magnet. The cesium was heated until it liquefied and flowed into the quartz tube.

Hydrogen gas was flowed through the quartz tube at 500 mtorr to generate a plasma with cesium vapor.

C. 407 nm Emission from Strontium and Ar^+ Catalyst

1.) The monochromator was under high vacuum with the valve to the cell closed. The cell was heated overnight at 275 °C corresponding to a filament power of 100 W. An argon-hydrogen mixture (97/3%) was flowed at 4 sccm through the cell port which maintained a total pressure of 1.5 torr. 2.) Next, the gas flow was stopped, and the cell pressure was reduced to less than 500 mtorr with the cell pump. The valve to the monochromator was opened. Both the cell pump and the spectrometer turbo pump were stopped so that the cell was no longer pumped. The argon-hydrogen mixture gas was added from the monochromator port. The flow rate was adjusted to achieve a pressure of 1 torr, and a 100 mtorr partial pressure of pure hydrogen was added by flowing the gas into the cell from the monochromator port until the total pressure was 1.1 torr. Since the valve to the monochromator was open, the entire light detection system was also at under the same gas as the cell. 3.) The filament power was increased to 200 W without pumping. When the temperature reached a steady state at 400 °C, the UV/VIS spectrum ($300-560\,nm$) was recorded with the photomultiplier tube (PMT) and the sodium salicylate scintillator (spectrum shown in Figure 20). 4.) Then the hydrogen pressure was increased to 10 torr by flowing pure hydrogen into the cell from the monochromator port. 5.) The power was increased to 300 W, and the cell was maintained at 600 °C overnight. 6.) Next, the cell pressure was reduced by pumping with the cell pump. When a pressure of 400 mtorr was achieved, the pumping was stopped. A strong blue-green plasma was observed. The UV/VIS spectrum ($300-560\,nm$) was recorded with the photomultiplier tube (PMT) and the sodium salicylate scintillator (spectrum shown in Figure 21). Without pumping the pressure gradually increased to about 1 torr. The plasma then ceased.

III. RESULTS

A. EUV Spectroscopy

The cell without any test material present was run to establish the baseline of the spectrometer. The intensity of the Lyman a emission as a function of time from the gas cell at a cell temperature of 700 °C comprising a tungsten filament, a titanium dissociator, and 300 mtorr hydrogen with a flow rate of 5.5 sccm is shown in Figure 2. The corresponding UV/VIS spectrum ($40-560\,nm$) is shown in Figure 3. The spectrum was recorded with a photomultiplier tube (PMT) and a sodium salicylate scintillator. No emission was observed except for the blackbody filament radiation at the longer wavelengths. No emission was also observed for the pure elements alone or when argon, neon, or helium replaced hydrogen.

The intensity of the Lyman a emission as a function of time from the gas cell at a cell temperature of 700 °C comprising a tungsten filament, a titanium dissociator, vaporized sodium, magnesium, or barium metal, and 300 mtorr hydrogen with a flow rate of 5.5 sccm are shown in Figures 4, 5, and 6, respectively. Sodium, magnesium, or barium metal was vaporized by filament heating. No emission was observed in any case. The maximum filament power was greater than 500 W. A metal coating formed in the cap of the cell over the course of the experiment in all cases.

The intensity of the Lyman a emission as a function of time from the gas cell at a cell temperature of 700 °C comprising a tungsten filament, a titanium dissociator, vaporized cesium or strontium metal, and 300 mtorr hydrogen with a flow rate of 5.5 sccm are shown in Figures 7 and 8, respectively. Strong emission was observed from both vaporized cesium and strontium with hydrogen. The EUV spectrum ($60-140\,nm$) of the cell emission recorded at about the point of the maximum Lyman a emission for cesium is shown in Figure 9. The EUV spectrum ($40-160\,nm$) of the cell emission recorded at about the point of the maximum Lyman a emission for strontium is shown in Figure 10. In each case, no emission was observed in the absence of hydrogen, and no emission occurred until

the catalyst was vaporized as indicated by the appearance of a metal coating in the cap of the cell over the course of the experiment.

Hydrogen was replaced by a 97% argon and 3% hydrogen mixture. The intensity of the Lyman a emission as a function of time from each gas cell was recorded. The intensity of the Lyman a emission as a function of time from the gas cell at a cell temperature of 700 °C comprising a tungsten filament, and 300 mtorr argon-hydrogen mixture (97/3%) that was recorded with a CEM is shown in Figure 11. No emission was observed with argon-hydrogen mixtures alone. The EUV spectrum ($40-160\,nm$) of the sodium, magnesium, and barium gas cell emission that was recorded with a PMT and a sodium salicylate scintillator two hours after the cell reached 700 °C are shown in Figures 12, 13, and 14, respectively. Each cell comprised a tungsten filament, vaporized metal, and 300 mtorr argon-hydrogen mixture (97/3%). No emission was observed in any case.

The EUV spectrum ($40-160\,nm$) of the cell emission recorded at about the point of the maximum Lyman a emission from the gas cell at a cell temperature of 700 °C comprising a tungsten filament, vaporized cesium or strontium metal, and 300 mtorr argon-hydrogen mixture (97/3%) with a flow rate of 5.5 sccm that was recorded with a PMT and a sodium salicylate scintillator are shown in Figures 15 and 16, respectively. Cesium or strontium metal was vaporized by filament heating. Strong emission was observed from both cesium and strontium with an argon-hydrogen mixture that was more intense than with hydrogen and cesium or strontium. The Lyman series corresponded to atomic hydrogen emission and strong Ar^+ ion emission was observed at 92.0 nm and 93.2 nm. The emission intensity of the plasma generated by the cesium or strontium catalyst increased significantly with the introduction of argon gas only when Ar^+ emission was observed.

The anomalous plasma required the presence of hydrogen. It was found that increasing the hydrogen pressure initially increased the atomic hydrogen emission lines, but with increasing hydrogen partial pressure at a constant total pressure, the Ar^+ emission in the EUV at 92.0 nm and 93.2 nm decreased which resulted in a decrease of the plasma intensity including the hydrogen emission. The zero order emission in the EUV was observed with titration of increasing partial pressure of

hydrogen added to argon gas. The optimum argon-hydrogen gas mixture which produced the greatest emission was determined to be 95% argon and 5% hydrogen.

Kuraica and Konjevic [38] observed intense $50\,eV$ anomalous thermal broadening of the Balmer lines with argon present in the negative glow of a glow discharge of an argon-hydrogen mixture irrespective of cathode material (carbon, copper, and silver), and an observed anomalous discharge was not observed in neon-hydrogen and pure hydrogen mixtures. The optimum argon-hydrogen gas mixture which produced the greatest emission in the present EUV study was similar to the 97% argon and 3% hydrogen mixture of Kuraica and Konjevic [38]. The optimum ratio was consistent with an anomalous discharge mechanism which required maximum concentrations of both atomic hydrogen and Ar^+.

B. EUV Emission of Ar^+ Catalyst Formed with Strontium

The EUV spectra ($40-160\,nm$) of the emission of a strontium-argon-hydrogen gas cell and a control hydrogen microwave plasma are shown in Figures 17, and 18, respectively. The standard EUV emission spectrum ($20-65\,nm$) of an argon microwave plasma recorded on the McPherson 4° grazing incidence EUV spectrometer (Model 248/310G) with a CEM is shown in Figure 19. A broad continuum radiation in the region of $45.6\,nm$ was observed in the strontium-argon-hydrogen gas cell emission that was not present in the control hydrogen or argon plasmas. (The broad continuum radiation in the region of $45.6\,nm$ shown in Figure 17 is actually significantly larger than shown due to the low grating efficiency at the short wavelengths.) This emission was dramatically different from that given by a microwave plasma of argon wherein the entire Rydberg series of lines of Ar^+ was observed with a discontinuity of the series at the limit of the ionization energy of Ar^+ to Ar^{2+} at $44.9\,nm$. In addition, an intense Rydberg series of lines in the region 110-130 nm was observed in the strontium-argon-hydrogen gas cell emission as shown in Figure 17. The lines were not present in the control hydrogen or argon plasmas, and were only observed with strontium present with argon and hydrogen.

The series was assigned to forbidden transitions of strontium which are not reported in the NIST Tables [39].

C. 407 nm Emission with Ar^+ Catalyst Formed with Strontium

The UV/VIS spectra ($300-560\,nm$) of the cell emission from the gas cell at a cell temperature of 400 °C comprising a tungsten filament, vaporized strontium metal, and 1.1 torr argon-hydrogen mixture (97/3%) following step #3 of the 407 Emission Protocol and step #5 of the 407 Emission Protocol are shown in Figures 20 and 21, respectively. The EUV spectra ($300-560\,nm$) of the cell emission from the strontium-argon-hydrogen gas cell following step #3 and step #5 of the 407 are superimposed in Figure 22. From the comparison, a novel continuum feature is observed at $407\,nm$ which was not due to strontium emission. The standard UV/VIS emission spectrum ($300-560\,nm$) of a hydrogen microwave plasma recorded on the McPherson model 302 (Seya-Namioka type) EUV spectrometer with a PMT and a sodium salicylate scintillator is shown in Figure 23. The EUV spectra ($300-560\,nm$) of the cell emission from the strontium-argon-hydrogen gas cell following step #5 of the 407 Emission Protocol and the standard hydrogen microwave plasma spectrum are superimposed in Figure 24. From the comparison, the novel $407\,nm$ continuum feature was not due to hydrogen emission. The novel $407\,nm$ continuum peak was observed by allowing the gas cell to react overnight under static conditions with strontium catalyst, a source of Ar^+ catalyst (argon gas), and excess hydrogen reactant. These results are consistent with the formation of $H^-(1/2)$ from the catalysis of atomic hydrogen by Ar^+. Unidentified continuum lines at 427.2 nm and 434.4 nm are indicated in Figure 21. These lines which are close to the 407 nm peak assigned to $H^-(1/2)$ may be due to resonant transfer from the hydride continuum emission to otherwise very weak strontium or hydrogen lines.

D. Broad 35-40 nm Peak with Ar^+ Catalyst

The EUV spectrum ($25-70\,nm$) of the cell emission from the gas cell at a cell temperature of 700 °C comprising a tungsten filament, vaporized

strontium metal, and 300 mtorr argon-hydrogen mixture (97/3%) is shown in Figure 25. A broad peak was observed in the 35-40 nm region. It coincided with strong Ar^+ emission wherein the Ar^+ was generated in the anomalous plasma formed by the atomic strontium catalyst. This peak may be due to an excimer of a highly excited argon ion, Ar^+, corresponding to the emission observed at 46 nm and the novel hydride ion, $H^-(1/2)$, corresponding to the emission observed at 407 nm. (See Discussion section.)

E. EUV Emission of Cesium Catalyst

The EUV spectrum ($40-160\,nm$) of the emission of the cesium-hydrogen gas cell is shown in Figures 26. Line emission corresponding to the second ionization energy of cesium, $23.15745\,eV$ [32], for the decay transition Cs^{2+} to Cs^+ was observed at $53.3\,nm$. (The $53.3\,nm$ emission shown in Figure 26 is actually significantly larger than shown due to the low grating efficiency at the short wavelengths.) The only cesium lines observed for the standard cesium microwave plasma were in the visible region, and no lines were observed at wavelengths shorter than $80\,nm$ in the case of the standard hydrogen microwave plasma as shown in Figure 18. The resonance lines of Cs II were observed with a sliding spark on the 10.7 m normal incidence vacuum spectrometer at the National Bureau of Standards (NBS) [40] as given in Table 1. The $53.3\,nm$ emission of the hydrogen catalysis reaction with cesium shown in Figure 26 is dramatically different from the NBS standard cesium spectrum wherein a series of lines of Cs^+ was observed that vanished at the limit of the ionization energy of Cs^+ to Cs^{2+}. In fact, the ionization limit was not observed; rather, it was derived by NBS to be $23.17(4)\,eV$ [40]. Furthermore, I. S. Aleksakhin et al. recorded the emission of cesium in the 45-75 nm region during electron-atom collisions [41]. The ionization energy limit at $53.3\,nm$ was not observed by I. S. Aleksakhin et al. either.

F. 407 nm Emission with Cesium Catalyst

The UV/VIS spectra ($300-560\,nm$) of the cesium-hydrogen gas cell ten minutes after the formation of a strong plasma and running

continuously for four hours since the formation of a strong plasma are shown in Figures 27 and 28, respectively. The noise features in Figure 27 at 425 nm and 480 nm were due to initial instabilities in the plasma as function of time. The UV/VIS spectra ($300-560\,nm$) of the cesium-hydrogen gas cell at the ten minute time point and the same cell at the four hour time point are superimposed in Figure 29. The UV/VIS spectrum ($300-560\,nm$) of the standard hydrogen microwave plasma is shown in Figure 23. The UV/VIS spectra ($300-560\,nm$) of the cesium-hydrogen gas cell at the four hour time point and the standard hydrogen microwave plasma are superimposed in Figure 30. From the comparison, a novel continuum feature is observed at $407\,nm$ which was not due to hydrogen or cesium emission. The novel $407\,nm$ continuum peak was observed only with cesium and atomic hydrogen present over an extended reaction time. These results are consistent with the formation of $H^-(1/2)$ from the catalysis of atomic hydrogen by $Cs(m)$.

G. 46 nm Emission with Ar^+ Catalyst Formed with Cesium

The EUV spectrum ($40-160\,nm$) of the emission of the cesium-argon-hydrogen gas cell, the cesium-hydrogen gas cell, and the hydrogen microwave plasma are shown in Figures 31, 26, and 18, respectively. The standard EUV emission spectrum ($20-65\,nm$) of an argon microwave plasma recorded on the McPherson 4° grazing incidence EUV spectrometer with a CEM is shown in Figure 19. A broad continuum radiation in the region of $45.6\,nm$ was observed in the cesium-argon-hydrogen gas cell emission that was not present in the cesium-hydrogen or control plasmas. This emission was dramatically different from that given by the argon microwave plasma wherein the entire Rydberg series of lines of Ar^+ was observed with a discontinuity of the series at the limit of the ionization energy of Ar^+ to Ar^{2+} at $44.9\,nm$ as shown in Figure 19. Thus, the novel $45.6\,nm$ continuum peak shown in Figure 31 for the case of Ar^+ catalyst formed by the anomalous plasma generated by strontium catalyst was observed with the addition of argon to the cesium-hydrogen plasma as shown in Figure 26. These results are consistent with the formation of Ar^+ which served as a second catalyst that was generated by the formation of a plasma with cesium catalyst.

IV. DISCUSSION

A plasma that emitted intense EUV formed at low temperatures (e.g. $\approx 10^3\ K$) from atomic hydrogen and atomic cesium or strontium catalyst which was vaporized from the metal by heating. The emission intensity of the plasma generated by the cesium or strontium catalyst increased significantly with the introduction of argon gas only when Ar^+ emission was observed. Ar^+ which served as a second catalyst was generated by the formation of a plasma with cesium or strontium catalyst. An intense Rydberg series of lines in the region 110-130 nm was assigned to forbidden transitions of strontium which are not reported in the NIST Tables [39]. The reason for the observation of the intense forbidden transitions may involve the strontium catalyst mechanism.

In the cases where Lyman a emission was observed, no possible chemical reactions of the tungsten filament, the dissociator, the vaporized test material, and 300 mtorr hydrogen or argon-hydrogen mixture gas at a cell temperature of 700 °C could be found which accounted for the hydrogen Lyman a line emission. In fact, no known chemical reaction releases enough energy to excite Lyman a emission from hydrogen. The emission was not observed with cesium, strontium, argon, hydrogen, or an argon-hydrogen mixture (97/3%) alone. Intense emission was observed for cesium and strontium with hydrogen gas and the argon-hydrogen mixture gas, but no emission was observed when sodium, magnesium, or barium replaced strontium or cesium with hydrogen or with the argon-hydrogen mixture. This result indicates that the emission was due to a reaction of the catalyst with hydrogen.

The only pure elements that were observed to emit EUV were those wherein the ionization of t electrons from an atom to a continuum energy level is such that the sum of the ionization energies of the t electrons is approximately $m \cdot 27.2\ eV$ where t and m are each an integer. Argon ions and cesium atoms ionize at an integer multiple of the potential energy of atomic hydrogen, $m \cdot 27.2\ eV$. The single ionization reaction ($t=1$) of Ar^+ to Ar^{2+} has a net enthalpy of reaction of $27.63\ eV$, which is equivalent to $m=1$. And, the double ionization ($t=2$) of Cs to Cs^{2+} has a net enthalpy of

reaction of $27.05135\,eV$, which is equivalent to $m=1$ [32]. In each case, the reaction involves a nonradiative energy transfer to form a hydrogen atom that is lower in energy than unreacted atomic hydrogen.

Characteristic emission was observed from a continuum state of Ar^{2+} which confirmed the resonate nonradiative energy transfer of $27.2\,eV$ from atomic hydrogen Ar^{+}. In the anomalous discharge of hydrogen due to the presence of Ar^{+}, atomic hydrogen may resonantly transfer energy to Ar^{+} to cause its ionization to Ar^{2+} which may then decay and emit the radiation. The vacuum reaction in the absence of an electric field is

$$Ar^{2+}+e^{-}\rightarrow Ar^{+}+27.63\,eV \tag{18}$$

In the catalysis of atomic hydrogen by Ar^{+}, a weak electric field may adjust the energy of ionizing Ar^{+} to Ar^{2+} to match the energy of $27.2\,eV$ to permit the catalysis. The transfer of $27.2\,eV$ from atomic hydrogen to Ar^{+} in the presence of the weak field of the filament results in its excitation to a continuum state. Then, the energy for the transition from essentially the Ar^{2+} state to the lowest state of Ar^{+} is predicted to give a broad continuum radiation in the region of $45.6\,nm$. This broad continuum emission was observed. This emission was dramatically different from that given by an argon microwave plasma wherein the entire Rydberg series of lines of Ar^{+} was observed with a discontinuity of the series at the limit of the ionization energy of Ar^{+} to Ar^{2+}. The observed Ar^{+} continuum in the region of $45.6\,nm$ confirms the catalyst mechanism of the anomalous discharge.

A broad peak observed in the 35-40 nm region is shown in Figure 25. It coincided with strong Ar^{+} emission wherein the Ar^{+} was generated in the anomalous plasma formed by the atomic strontium catalyst. This peak may be due to an excimer of a highly excited argon ion, Ar^{+}, corresponding to the emission observed at 46 nm and the novel hydride ion, $H^{-}(1/2)$, corresponding to the emission observed at 407 nm. Ar^{+} is excited to the bound-free limit during the catalysis of atomic hydrogen, and $H^{-}(1/2)$ is formed in its bound-free state by the reaction of the hydrogen catalysis product with an electron.

$$H(1/2)+e^{-}\rightarrow H^{-}(1/2) \tag{19}$$

In addition, the hydride high energy states are easily excited due to the continuum absorption feature of any hydride ion. The argon ion and the

high binding energy hydride ion may form an excimer that is similar to an argon monohalide excimer.

Broad peaks due to excimers of argon and the halides chlorine and fluorine are known to emit at much longer wavelengths and are the basis of argon halogen excimer lasers [42]. Excimer lasers involve emission from an excited molecule which dissociates following the emission due to a repulsive potential curve between the unexcited atoms. For the hypothetical excimer molecule AB, collision of unexcited A and B atoms occurs along a repulsive potential curve. However, if the electrons in one atom such as B are excited, creating a state labeled B^*, B^* may combine with atom A to produce an excited state of the molecule AB^*. Binding energies, relative to excited atoms, for such excited state complexes range from $0.1\,eV$ for many rare gas-metal atom combinations, to about $5\,eV$ for noble gas monohalides [42].

In excimer lasers, the pumping is by direct electron beam pumping, electron-beam-controlled-discharge pumping, and self-sustained-discharge pumping [43]. Pumping reactions include

$$Ar^+ + F^- + Ar \rightarrow ArF^{*"} + Ar \tag{20}$$

$$Ar_2^+ + F^- + Ar \rightarrow ArF^{*"} + 2Ar \tag{21}$$

$$Ar^* + F_2 \rightarrow ArF^* + F \tag{22}$$

$$Ar_2^* + F_2 \rightarrow ArF^* + Ar + F \tag{23}$$

where $ArF^{*"}$ denotes the ionic excited states of ArF with large amounts of vibrational excitation. In the case of the $ArCl$ excimer laser, the 170 nm continuum band emission has been determined to be due to an ionic excited state of argon monochloride, Ar^+Cl^-, emitting to the repulsive $ArCl$ ground state [42].

The broad peak starting at 40 and ending at about 35 nm may be the ionic pair excimer emission of Ar^{+**} and $H^{-**}(1/2)$. (A highly excited state of a species M at the bound-free limit is represented by the M^{**}.) This peak has an energy width of about $4.5\,eV$ which is about the typical binding energy, relative to excited atoms, for such excited state noble gas monohalides complexes. Possible excimer reactions with emission that match the observed peak starting at 40 nm are

$$Ar^{+**} + H^{-**}(1/2) \rightarrow ArH(1/2)^{**} \rightarrow Ar + H(1/2) + 30.66\ eV\ (40.45nm) \quad (24)$$

$$Ar^{+**} + H^{-**}(1/2) \rightarrow ArH(1/2)^{**} \rightarrow Ar^{+} + H^{-}(1/2) + 30.66\ eV\ (40.45nm) \quad (25)$$

Rather than requiring energy intensive electron beam or discharge pumping schemes, the plasma and the excimer are formed by the catalysis of atomic hydrogen with the potential for a very short wavelength, energy efficient excimer laser.

Characteristic Cs^{2+} line emission was observed which confirmed the resonate nonradiative energy transfer of $27.2\ eV$ from atomic hydrogen to atomic cesium. In the anomalous discharge of hydrogen due to the presence of atomic cesium, atomic hydrogen may resonantly transfer energy to cesium to cause its double ionization to Cs^{2+} which may then decay and emit the radiation. The vacuum reaction is

$$Cs^{2+} + e^{-} \rightarrow Cs^{+} + 23.2\ eV \quad (26)$$

In the catalysis of atomic hydrogen by cesium, thermal energies may broaden the enthalpy of reaction. The relationship between kinetic energy and temperature is given by

$$E_{kinetic} = \frac{3}{2}kT \quad (27)$$

For a temperature of 1200 K, the thermal energy is 0.16 eV, and the net enthalpy of reaction provided by cesium metal is 27.21 eV which matches the energy of $27.2\ eV$ to permit the catalysis. Following the resonant transfer, the decay energy for the transition Cs^{2+} to Cs^{+} is predicted to give $27.2\ eV$ line emission corresponding to the second ionization energy of cesium, $23.15745\ eV$. This line emission was observed. This emission was dramatically different from that given by a microwave plasma of argon wherein the entire Rydberg series of lines of Cs^{+} was observed with a discontinuity of the series at the limit of the ionization energy of Cs^{+} to Cs^{2+}. The observed Cs^{2+} single line emission at $53.3\ nm$ confirms the catalyst mechanism of the anomalous discharge.

$Cs(m)$ and Ar^{2+} are predicted to catalyze hydrogen to form $H\left[\frac{a_H}{2}\right]$ which reacts with and electron to form $H^{-}(1/2)$. The predicted $H^{-}(1/2)$ hydride ion of hydrogen catalysis by either cesium atom or Ar^{+} catalyst

was observed spectroscopically at 407 *nm* corresponding to its predicted binding energy of 3.05 *eV*. The hydride reaction product formed over time.

The release of energy from hydrogen as evidenced by the EUV emission must result in a lower-energy state of hydrogen. The present study identified the formation of a novel hydride ion The formation of novel compounds based on novel hydride ions would be substantial evidence supporting catalysis of hydrogen as the mechanism of the observed EUV emission and further support the present spectroscopic identification of $H^-(1/2)$. Compounds containing hydrino hydride ions have been isolated as products of the reaction of atomic hydrogen with atoms and ions identified as catalysts in this and previously reported EUV studies [12, 14-31]. The novel hydride compounds were identified analytically by techniques such as time of flight secondary ion mass spectroscopy, X-ray photoelectron spectroscopy, and ^1H nuclear magnetic resonance spectroscopy. For example, the time of flight secondary ion mass spectroscopy showed a large hydride peak in the negative spectrum. The X-ray photoelectron spectrum showed large metal core level shifts due to binding with the hydride as well as novel hydride peaks. The ^1H nuclear magnetic resonance spectrum showed significantly upfield shifted peaks which corresponded to and identified novel hydride ions. The implications are that a new field of novel hydrogen chemistry has been discovered.

ACKNOWLEDGMENT

Special thanks to Ying Lu, Takeyoshi Onuma, and Jiliang He for recording the spectra and Bala Dhandapani for assisting with logistics and reviewing this manuscript.

REFERENCES

1. R. Mills, The Grand Unified Theory of Classical Quantum Mechanics, January 2000 Edition, BlackLight Power, Inc., Cranbury, New Jersey, Distributed by Amazon.com.

2. R. Mills, N. Greenig, S. Hicks, "Optically Measured Power Balances of Anomalous Discharges of Mixtures of Argon, Hydrogen, and Potassium, Rubidium, Cesium, or Strontium Vapor", Int. J. Hydrogen Energy, submitted.
3. R. Mills and M. Nansteel, "Anomalous Argon-Hydrogen-Strontium Discharge", IEEE Transactions of Plasma Science, submitted.
4. R. Mills, M. Nansteel, and Y. Lu, "Anomalous Hydrogen-Strontium Discharge", European Journal of Physics D, submitted.
5. R. Mills, J. Dong, Y. Lu, "Observation of Extreme Ultraviolet Hydrogen Emission from Incandescently Heated Hydrogen Gas with Certain Catalysts", Int. J. Hydrogen Energy, Vol. 25, (2000), pp. 919-943.
6. R. Mills, "Observation of Extreme Ultraviolet Emission from Hydrogen-KI Plasmas Produced by a Hollow Cathode Discharge", Int. J. Hydrogen Energy, in press.
7. R. Mills, "Temporal Behavior of Light-Emission in the Visible Spectral Range from a Ti-K2CO3-H-Cell", Int. J. Hydrogen Energy, in press.
8. R. Mills, Y. Lu, and T. Onuma, "Formation of a Hydrogen Plasma from an Incandescently Heated Hydrogen-Catalyst Gas Mixture with an Anomalous Afterglow Duration", Int. J. Hydrogen Energy, in press.
9. R. Mills, M. Nansteel, and Y. Lu, "Observation of Extreme Ultraviolet Hydrogen Emission from Incandescently Heated Hydrogen Gas with Strontium that Produced an Anomalous Optically Measured Power Balance", Int. J. Hydrogen Energy, in press.
10. R. Mills, J. Dong, Y. Lu, J. Conrads, "Observation of Extreme Ultraviolet Hydrogen Emission from Incandescently Heated Hydrogen Gas with Certain Catalysts", 1999 Pacific Conference on Chemistry and Spectroscopy and the 35th ACS Western Regional Meeting, Ontario Convention Center, California, (October 6-8, 1999).
11. R. Mills, J. Dong, N. Greenig, and Y. Lu, "Observation of Extreme Ultraviolet Hydrogen Emission from Incandescently Heated Hydrogen Gas with Certain Catalysts", National Hydrogen Association, 11 th Annual U.S. Hydrogen Meeting, Vienna, VA, (February 29-March 2, 2000).
12. R. Mills, B. Dhandapani, N. Greenig, J. He, J. Dong, Y. Lu, and H. Conrads, "Formation of an Energetic Plasma and Novel Hydrides from Incandescently Heated Hydrogen Gas with Certain Catalysts", National

Hydrogen Association, 11 th Annual U.S. Hydrogen Meeting, Vienna, VA, (February 29-March 2, 2000).
13. Mills, J. Dong, N. Greenig, and Y. Lu, "Observation of Extreme Ultraviolet Hydrogen Emission from Incandescently Heated Hydrogen Gas with Certain Catalysts", 219 th National ACS Meeting, San Francisco, California, (March 26-30, 2000).
14. R. Mills, B. Dhandapani, N. Greenig, J. He, J. Dong, Y. Lu, and H. Conrads, "Formation of an Energetic Plasma and Novel Hydrides from Incandescently Heated Hydrogen Gas with Certain Catalysts", 219 th National ACS Meeting, San Francisco, California, (March 26-30, 2000).
15. R. Mills, B. Dhandapani, N. Greenig, J. He, J. Dong, Y. Lu, and H. Conrads, "Formation of an Energetic Plasma and Novel Hydrides from Incandescently Heated Hydrogen Gas with Certain Catalysts", June ACS Meeting (29th Northeast Regional Meeting, University of Connecticut, Storrs, CT, (June 18-21, 2000)).
16. R. Mills, B. Dhandapani, N. Greenig, J. He, J. Dong, Y. Lu, and H. Conrads, "Formation of an Energetic Plasma and Novel Hydrides from Incandescently Heated Hydrogen Gas with Certain Catalysts", August National ACS Meeting (220th ACS National Meeting, Washington, DC, (August 20-24, 2000)).
17. R. Mills, B. Dhandapani, N. Greenig, J. He, "Synthesis and Characterization of Potassium Iodo Hydride", Int. J. of Hydrogen Energy, Vol. 25, Issue 12, December, (2000), pp. 1185-1203.
18. R. Mills, "Novel Inorganic Hydride", Int. J. of Hydrogen Energy, Vol. 25, (2000), pp. 669-683.
19. R. Mills, "Novel Hydrogen Compounds from a Potassium Carbonate Electrolytic Cell", Fusion Technology, Vol. 37, No. 2, March, (2000), pp. 157-182.
20. R. Mills, B. Dhandapani, M. Nansteel, J. He, T. Shannon, A. Echezuria, "Synthesis and Characterization of Novel Hydride Compounds", Int. J. of Hydrogen Energy, in press.
21. R. Mills, B. Dhandapani, M. Nansteel, J. He, A. Voigt, "Identification of Compounds Containing Novel Hydride Ions by Nuclear Magnetic Resonance Spectroscopy", Int. J. Hydrogen Energy, submitted.
22. R. Mills, "Highly Stable Novel Inorganic Hydrides", Journal of Materials Research, submitted.

23. R. Mills, "Novel Hydride Compound", 1999 Pacific Conference on Chemistry and Spectroscopy and the 35th ACS Western Regional Meeting, Ontario Convention Center, California, (October 6-8, 1999).
24. R. Mills, B, Dhandapani, N. Greenig, J. He, "Synthesis and Characterization of Potassium Iodo Hydride", 1999 Pacific Conference on Chemistry and Spectroscopy and the 35th ACS Western Regional Meeting, Ontario Convention Center, California, (October 6-8, 1999).
25. R. Mills, J. He, and B. Dhandapani, "Novel Hydrogen Compounds", 1999 Pacific Conference on Chemistry and Spectroscopy and the 35th ACS Western Regional Meeting, Ontario Convention Center, California, (October 6-8, 1999).
26. R. Mills, "Novel Hydride Compound", National Hydrogen Association, 11 th Annual U.S. Hydrogen Meeting, Vienna, VA, (February 29-March 2, 2000).
27. R. Mills, J. He, and B. Dhandapani, "Novel Alkali and Alkaline Earth Hydrides", National Hydrogen Association, 11 th Annual U.S. Hydrogen Meeting, Vienna, VA, (February 29-March 2, 2000).
28. R. Mills, "Novel Hydride Compound", 219 th National ACS Meeting, San Francisco, California, (March 26-30, 2000).
29. R. Mills, J. He, and B. Dhandapani, "Novel Alkali and Alkaline Earth Hydrides", 219 th National ACS Meeting, San Francisco, California, (March 26-30, 2000).
30. R. Mills, J. He, and B. Dhandapani, "Novel Alkali and Alkaline Earth Hydrides", August National ACS Meeting (220 th ACS National Meeting, Washington, DC, (August 20-24, 2000)).
31. R. Mills, W. Good, A. Voigt, Jinquan Dong, "Minimum Heat of Formation of Potassium Iodo Hydride", Int. J. Hydrogen Energy, submitted.
32. David R. Linde, *CRC Handbook of Chemistry and Physics*, 79 th Edition, CRC Press, Boca Raton, Florida, (1998-9), p. 10-175 to p. 10-177.
33. R. Mills, The Nature of Free Electrons in Superfluid Helium--a Test of Quantum Mechanics and a Basis to Review its Foundations and Make a Comparison to Classical Theory, Int. J. Hydrogen Energy, in press.
34. R. Mills, "The Hydrogen Atom Revisited", Int. J. of Hydrogen Energy, Vol. 25, Issue 12, December, (2000), pp. 1171-1183.
35. N. V. Sidgwick, *The Chemical Elements and Their Compounds*, Volume I, Oxford, Clarendon Press, (1950), p.17.

36. M. D. Lamb, *Luminescence Spectroscopy*, Academic Press, London, (1978), p. 68.
37. C. L. Yaws, *Chemical Properties Handbook*, McGraw-Hill, (1999).
38. Kuraica, M., Konjevic, N., Physical Review A, Volume 46, No. 7, October (1992), pp. 4429-4432.
39. NIST Atomic Spectra Database, www.physics.nist.gov/cgi-bin/AtData/display.ksh.
40. J. Reader, G. L. Epstein, "Resonance lines of Cs II, Ba II, and La IV", Journal of the Optical Society of America, Vol. 65, No. 6, June, (1975), pp. 638-641.
41. I. S. Aleksakhin, G. G. Bogachev, A. I. Zapesochnyi, "Study of the emission of potassium, rubidium, and cesium in the 45-75 nm region during electron-atom collisions", J. Applied Spectroscopy, Vol. 23, No. 6, December, (1975), pp. 1666-1668. Translated from Zh. Prikl. Spektrosk. (USSR), Vol. 23, No. 6, December (1975), pp. 1103-1105.
42. J. J. Ewing. "Excimer Lasers", *Laser Handbook*, Edited by M. L. Stitch, North-Holland Publishing Company, Vol. A4, (1979) , pp. 135-197.
43. H. Shimazaki, S. Nakamura, M. Obara, T. Fujioka, AIP Conference Proceedings, Series Editor: H. C. Wolfe, No. 100, Subseries in Optical Science and Engineering, No. 3, Excimer Lasers-1983, Edited by C. I. Rhodes, H. Egger, H. Pummer, OSA, Lake Tahoe, Nevada, American Institute of Physics, New York, (1983), pp. 12-18.

Table 1. Resonance lines of Cs II observed with a sliding spark on the 10.7 m normal incidence vacuum spectrometer at NBS [40]. The uncertainty of the wavelengths is ±0.005 Å.

λ (Å)	Intensity	σ (cm^{-1})	Upper Level
926.657	40000	107914.8	$6p^6 5d\ ^3P_1$
901.270	35000	110954.5	$6s3/2[3/2]_1$
813.837	15000	122874.7	$6s1/2[1/2]_1$
808.761	15000	123645.9	$5d\ ^3D_1$
718.138	15000	139249.0	$5d\ ^1P_1$
668.386	500	149614	$7s3/2[3/2]_1$
657.112	100	152181	$6d\ ^3P_1$
639.356	2000	156407	$6d\ ^3D_1$
612.756	35	163189	$7s1/2[1/2]_1$
591.044	250	169192	$6d\ ^1P_1$
607.291	50	164666	$8s3/2[3/2]_1$
575.320	10	173816	$6d\ ^3D_1$
564.158	1	177256	$7d\ ^1P_1$

Figure Captions

Figure 1. The experimental set up comprising a gas cell light source and an EUV spectrometer which was differentially pumped.

Figure 2. The intensity of the Lyman α emission as a function of time from the gas cell at a cell temperature of 700 °C comprising a tungsten filament, a titanium dissociator, and 300 mtorr hydrogen that was recorded with a CEM.

Figure 3. The UV/VIS spectrum ($40-560\,nm$) of the cell emission from the gas cell at a cell temperature of 700 °C comprising a tungsten filament, a titanium dissociator, and 300 mtorr hydrogen that was recorded with a photomultiplier tube (PMT) and a sodium salicylate scintillator with slit widths of $500X500\,\mu m$.

Figure 4. The intensity of the Lyman α emission as a function of time from the gas cell at a cell temperature of 700 °C comprising a tungsten filament, a titanium dissociator, vaporized sodium metal, and 300 mtorr hydrogen that was recorded with a CEM.

Figure 5. The intensity of the Lyman α emission as a function of time from the gas cell at a cell temperature of 700 °C comprising a tungsten filament, a titanium dissociator, vaporized magnesium, and 300 mtorr hydrogen that was recorded with a CEM.

Figure 6. The intensity of the Lyman α emission as a function of time from the gas cell at a cell temperature of 700 °C comprising a tungsten filament, a titanium dissociator, vaporized barium metal, and 300 mtorr hydrogen that was recorded with a CEM.

Figure 7. The intensity of the Lyman α emission as a function of time from the gas cell at a cell temperature of 700 °C comprising a tungsten filament, a titanium dissociator, vaporized cesium metal, and 300 mtorr hydrogen that was recorded with a CEM.

Figure 8. The intensity of the Lyman α emission as a function of time from the gas cell at a cell temperature of 700 °C comprising a tungsten filament, a titanium dissociator, vaporized strontium metal, and 300 mtorr hydrogen that was recorded with a CEM.

Figure 9. The EUV spectrum ($60-140\,nm$) of the cell emission recorded at about the point of the maximum Lyman α emission from the gas cell at a cell temperature of 700 °C comprising a tungsten filament, a

titanium dissociator, vaporized cesium metal, and 300 mtorr hydrogen that was recorded with a CEM.

Figure 10. The EUV spectrum (40 – 160 *nm*) of the cell emission recorded at about the point of the maximum Lyman α emission from the gas cell at a cell temperature of 700 °C comprising a tungsten filament, a titanium dissociator, vaporized strontium metal, and 300 mtorr hydrogen that was recorded with a CEM.

Figure 11. The intensity of the Lyman α emission as a function of time from the gas cell at a cell temperature of 700 °C comprising a tungsten filament, and 300 mtorr argon-hydrogen mixture (97/3%) that was recorded with a CEM.

Figure 12. The EUV emission spectrum (40 – 160 *nm*) from a gas cell comprising a tungsten filament, vaporized sodium metal, and 300 mtorr argon-hydrogen mixture (97/3%) that was recorded with a PMT and a sodium salicylate scintillator two hours after the cell reached 700 °C.

Figure 13. The EUV emission spectrum (40 – 160 *nm*) from a gas cell comprising a tungsten filament, vaporized magnesium metal, and 300 mtorr argon-hydrogen mixture (97/3%) that was recorded with a PMT and a sodium salicylate scintillator two hours after the cell reached 700 °C.

Figure 14. The EUV emission spectrum (40 – 160 *nm*) from a gas cell comprising a tungsten filament, vaporized barium metal, and 300 mtorr argon-hydrogen mixture (97/3%) that was recorded with a PMT and a sodium salicylate scintillator two hours after the cell reached 700 °C.

Figure 15. The EUV spectrum (40 – 160 *nm*) of the cell emission recorded at about the point of the maximum Lyman α emission from the gas cell at a cell temperature of 700 °C comprising a tungsten filament, vaporized cesium metal, and 300 mtorr argon-hydrogen mixture (97/3%) that was recorded with a PMT and a sodium salicylate scintillator.

Figure 16. The EUV spectrum (40 – 160 *nm*) of the cell emission recorded at about the point of the maximum Lyman α emission from the gas cell at a cell temperature of 700 °C comprising a tungsten filament, vaporized strontium metal, and 300 mtorr argon-hydrogen mixture (97/3%) that was recorded with a PMT and a sodium salicylate scintillator.

Figure 17. The EUV spectrum (40 – 160 *nm*) of the cell emission from

the gas cell at a cell temperature of 700 °C comprising a tungsten filament, vaporized strontium metal, and 300 mtorr argon-hydrogen mixture (97/3%) that showed novel catalysts features and spectral lines.

Figure 18. Standard EUV emission spectrum (40 – 160 *nm*) of a hydrogen microwave plasma recorded on the McPherson model 302 (Seya-Namioka type) EUV spectrometer with a PMT and a sodium salicylate scintillator.

Figure 19. Standard EUV emission spectrum (20 – 65 *nm*) of an argon microwave plasma recorded on the McPherson 4° grazing incidence EUV spectrometer (Model 248/310G) with a CEM.

Figure 20. The EUV spectrum (300 – 560 *nm*) of the cell emission from the gas cell at a cell temperature of 400 °C comprising a tungsten filament, vaporized strontium metal, and 1.1 torr argon-hydrogen mixture (97/3%) following step #3 of the 407 Emission Protocol that was recorded with a PMT and a sodium salicylate scintillator.

Figure 21. The UV/VIS spectrum (300 – 560 *nm*) of the cell emission from the gas cell at a cell temperature of 600 °C comprising a tungsten filament, vaporized strontium metal, and 400 mtorr argon-hydrogen mixture (97/3%) following step #5 of the 407 Emission Protocol that was recorded with a PMT and a sodium salicylate scintillator.

Figure 22. The EUV spectra (300 – 560 *nm*) of the cell emission from the strontium-argon-hydrogen gas cell following step #3 (dotted line) and step #5 (solid line) of the 407 Emission Protocol.

Figure 23. Standard UV/VIS emission spectrum (300 – 560 *nm*) of a hydrogen microwave plasma recorded on the McPherson model 302 (Seya-Namioka type) EUV spectrometer with a PMT and a sodium salicylate scintillator.

Figure 24. The UV/VIS spectra (300 – 560 *nm*) of the cell emission from strontium-argon-hydrogen gas cell following step #5 (solid line) of the 407 Emission Protocol and the standard hydrogen microwave plasma (dotted line).

Figure 25. The EUV spectrum (25 – 70 *nm*) of the cell emission from the gas cell at a cell temperature of 700 °C comprising a tungsten filament, vaporized strontium metal, and 300 mtorr argon-hydrogen mixture (97/3%) that was recorded with a CEM.

Figure 26. The EUV spectrum (40 – 160 *nm*) of the cell emission from

the gas cell at a cell temperature of 700 °C comprising a tungsten filament, vaporized cesium metal, and 300 mtorr hydrogen that was recorded with a PMT and a sodium salicylate scintillator.

Figure 27. The UV/VIS spectrum ($300-560\,nm$) of the cell emission from the gas cell that was recorded with a PMT and a sodium salicylate scintillator ten minutes after the formation of a strong plasma. The cell at 700 °C comprised a tungsten filament, vaporized cesium metal, and 300 mtorr hydrogen.

Figure 28. The UV/VIS spectrum ($300-560\,nm$) of the cell emission from the gas cell that was recorded with a PMT and a sodium salicylate scintillator four hours after the formation of a sustained strong plasma. The cell at 700 °C comprised a tungsten filament, vaporized cesium metal, and 300 mtorr hydrogen.

Figure 29. The UV/VIS spectra ($300-560\,nm$) of the cesium-hydrogen gas cell at the ten minute time point (dotted line) and same the cell at the four hour time point (solid line).

Figure 30. The UV/VIS spectra ($300-560\,nm$) of the cell emission from cesium-hydrogen gas cell at the four hour time point and the standard hydrogen microwave plasma.

Figure 31. The EUV spectrum ($40-160\,nm$) of the cell emission from the gas cell at a cell temperature of 700 °C comprising a tungsten filament, vaporized cesium metal, and 300 mtorr argon-hydrogen mixture (97/3%) that was recorded with a CEM with a MgF_2 coated grating.

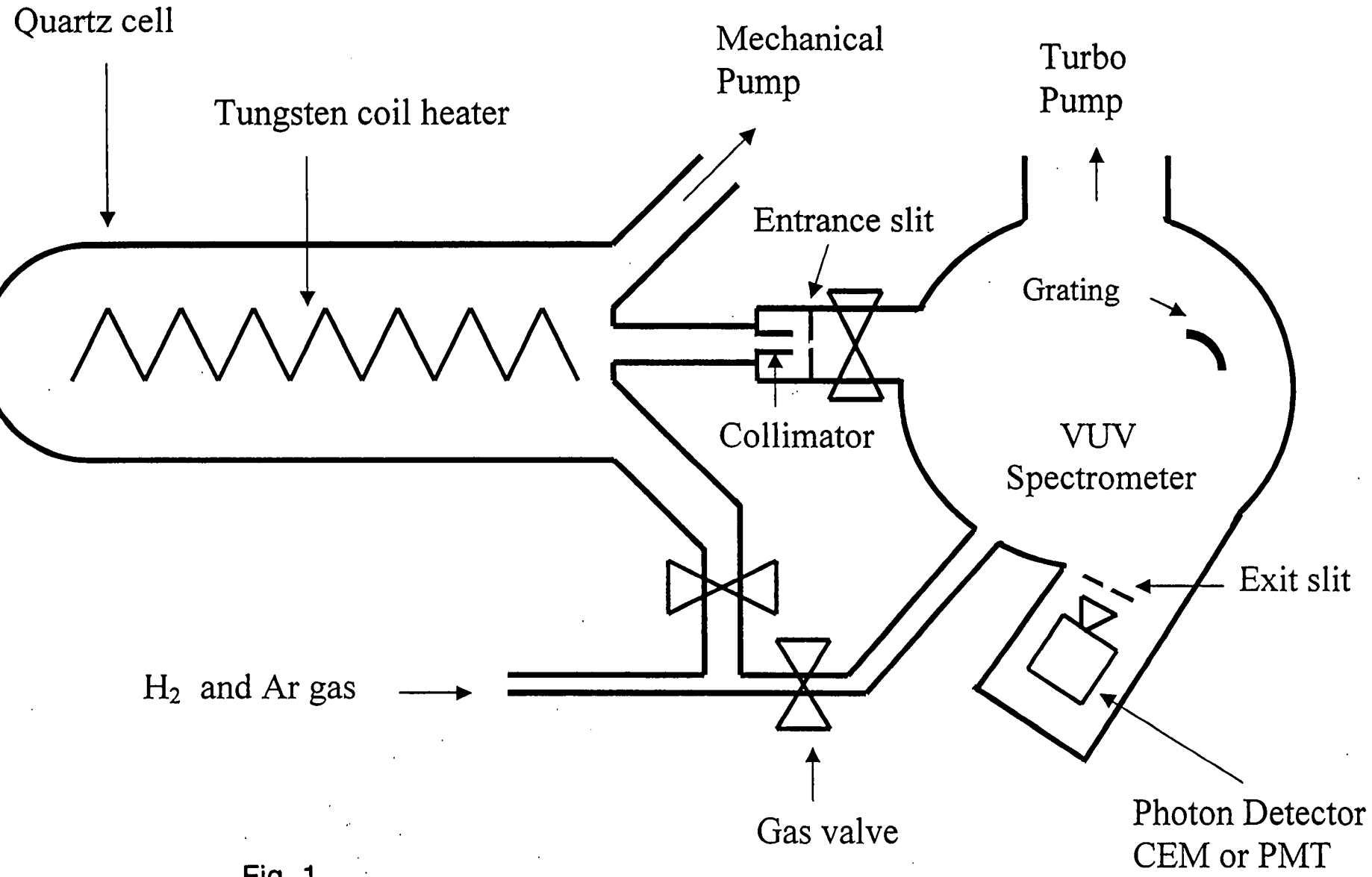
Quartz cell
Tungsten coil heater
Mechanical Pump
Turbo Pump
Entrance slit
Grating
Collimator
VUV Spectrometer
Exit slit
H_2 and Ar gas
Gas valve
Photon Detector CEM or PMT

Fig. 1

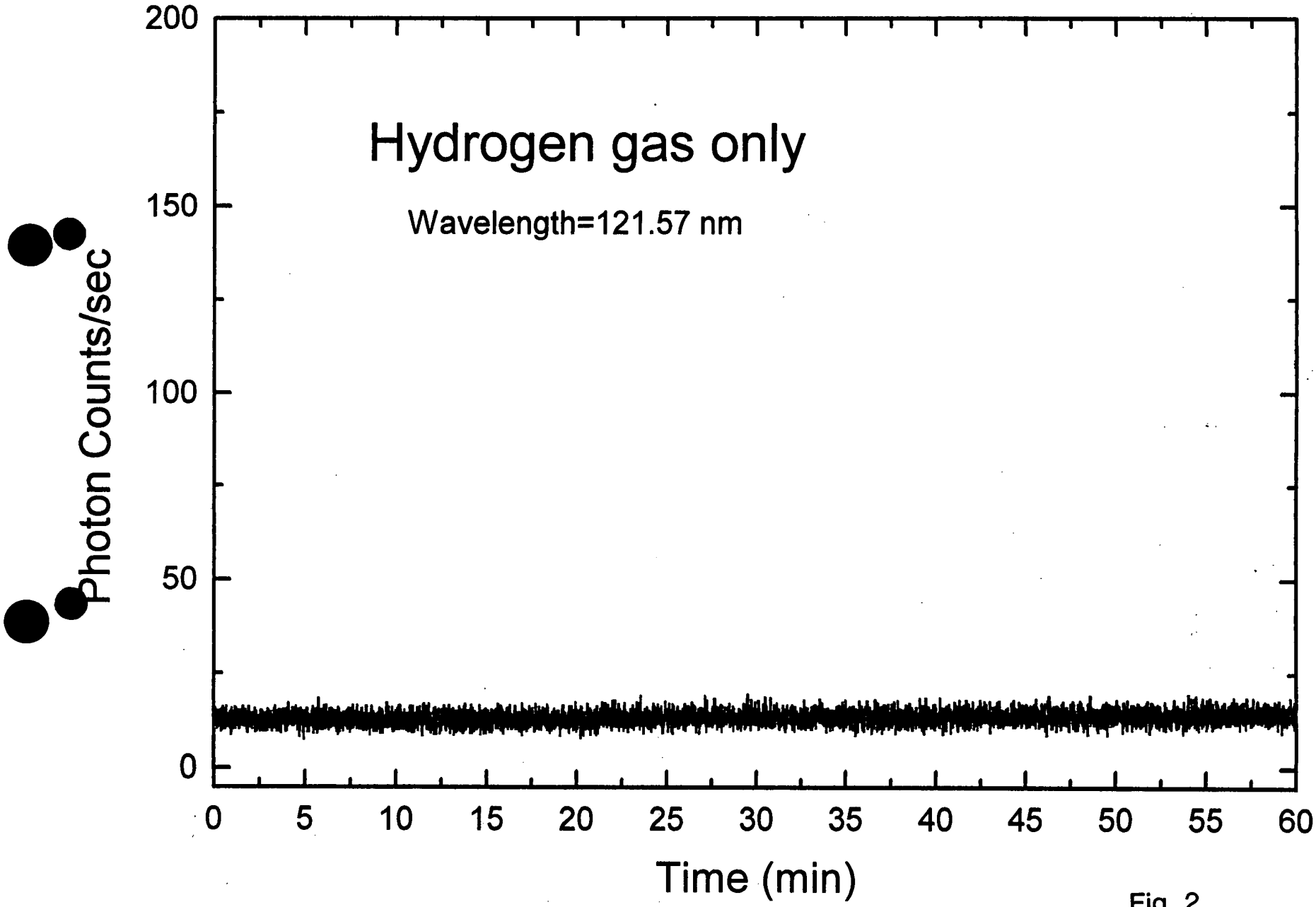
Hydrogen gas only
Wavelength=121.57 nm
Photon Counts/sec
200
150
100
50
0
0
5
10
15
20
25
30
35
40
45
50
55
60
Time (min)

Fig. 2

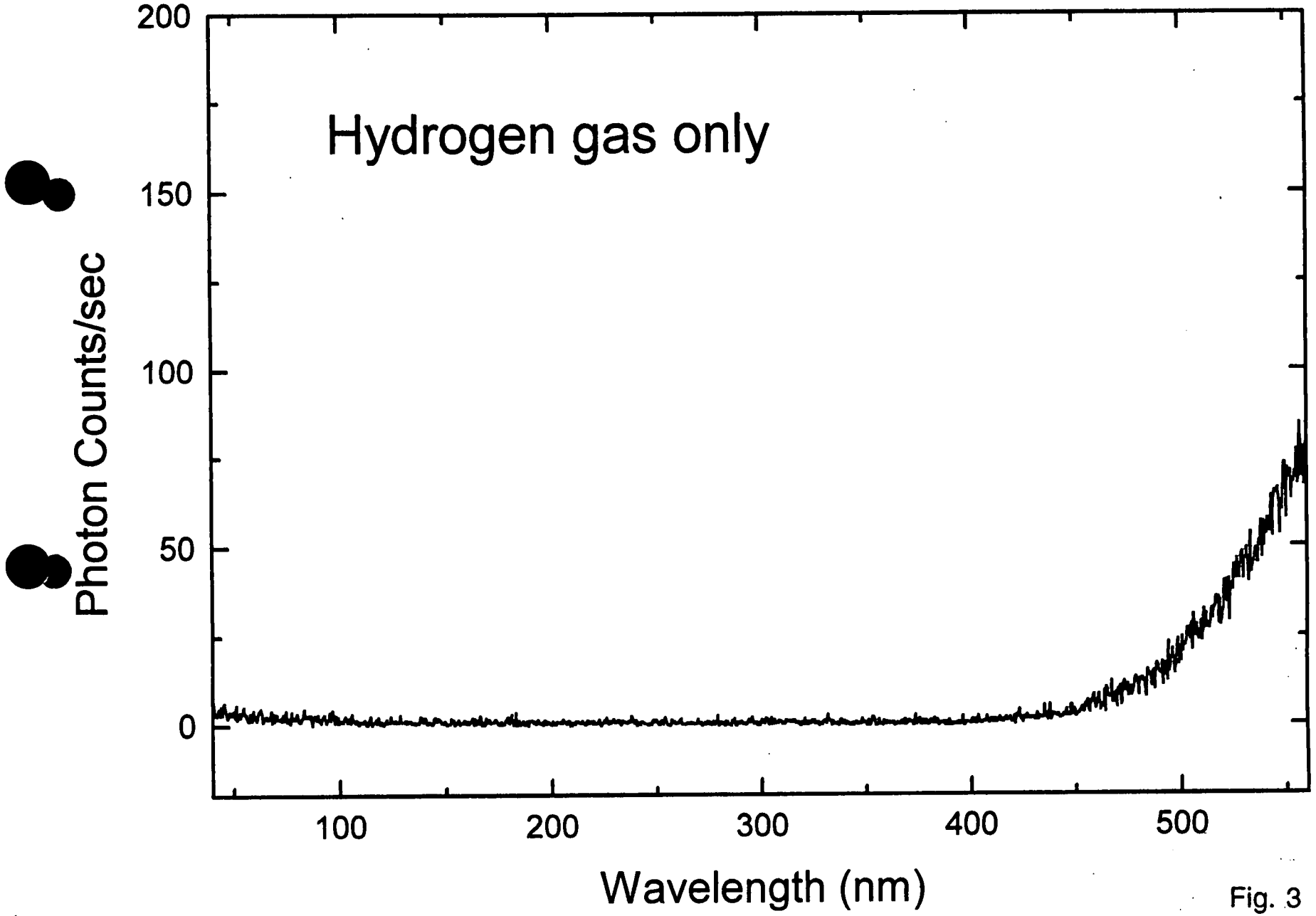
Hydrogen gas only
Photon Counts/sec
200
150
100
50
0
100
200
300
400
500
Wavelength (nm)

Fig. 3

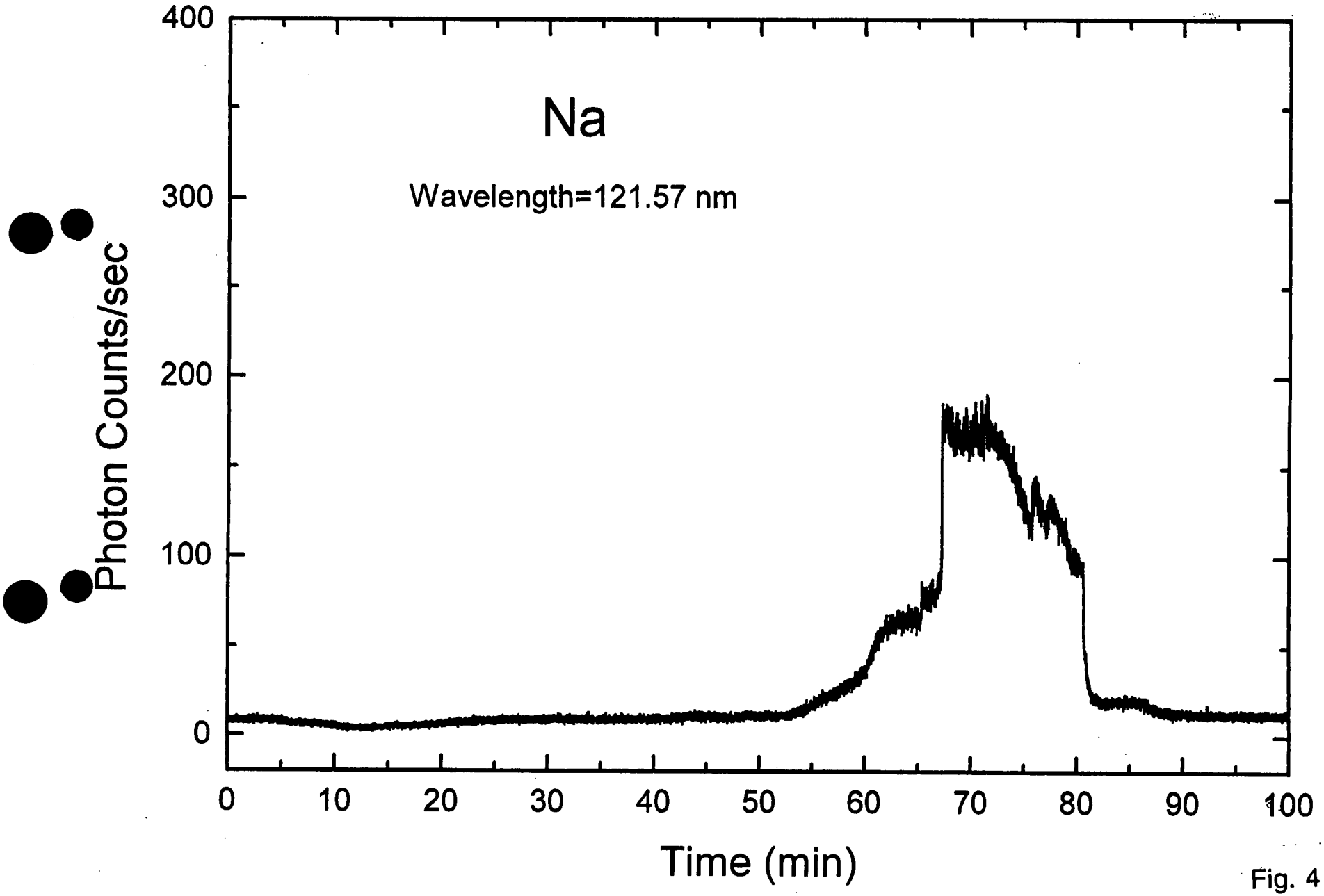
Na
Wavelength=121.57 nm
Photon Counts/sec
Time (min)
400
300
200
100
0
0
10
20
30
40
50
60
70
80
90
100

Fig. 4

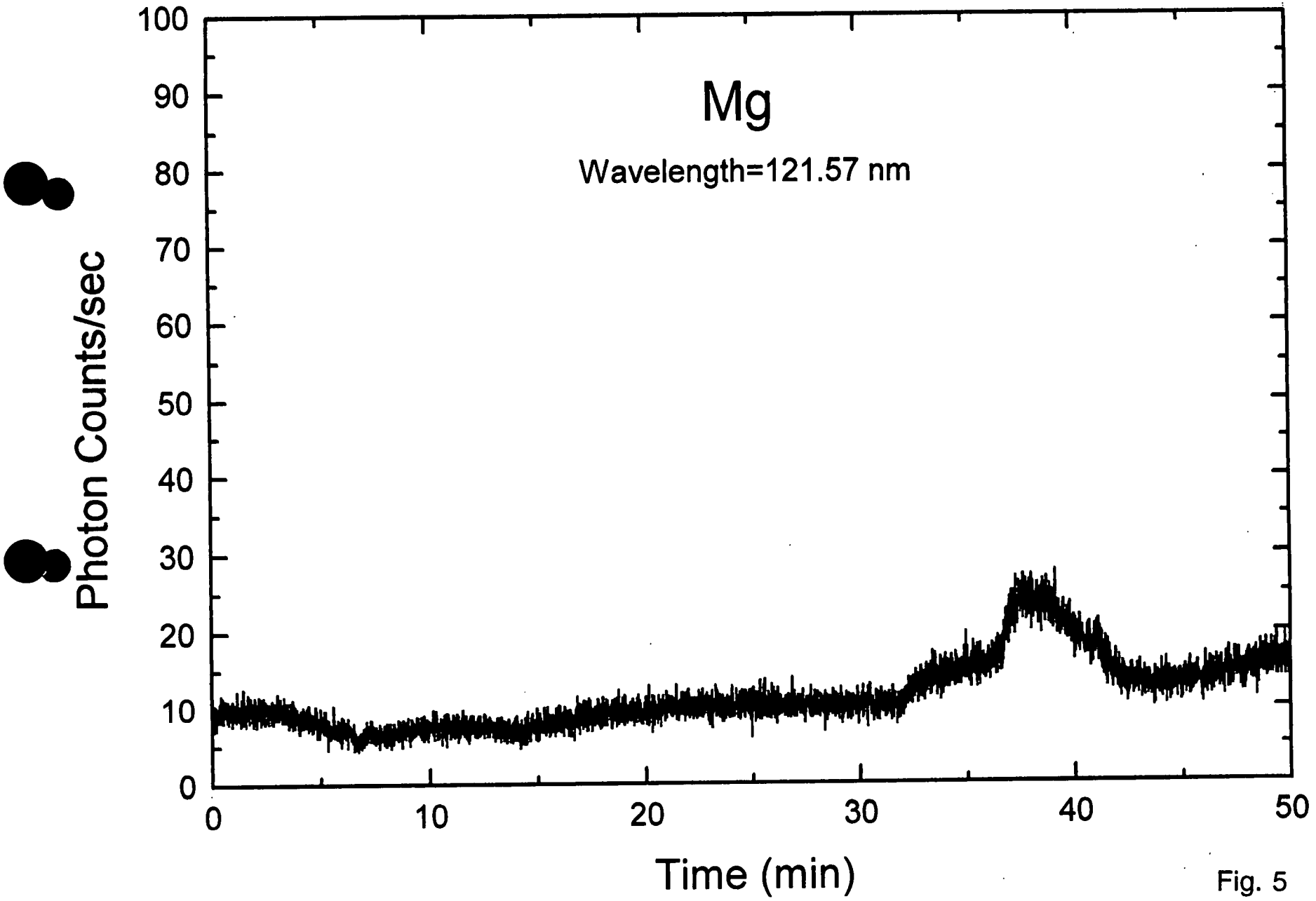
Mg
Wavelength=121.57 nm
Photon Counts/sec
Time (min)
0
10
20
30
40
50
60
70
80
90
100

Fig. 5

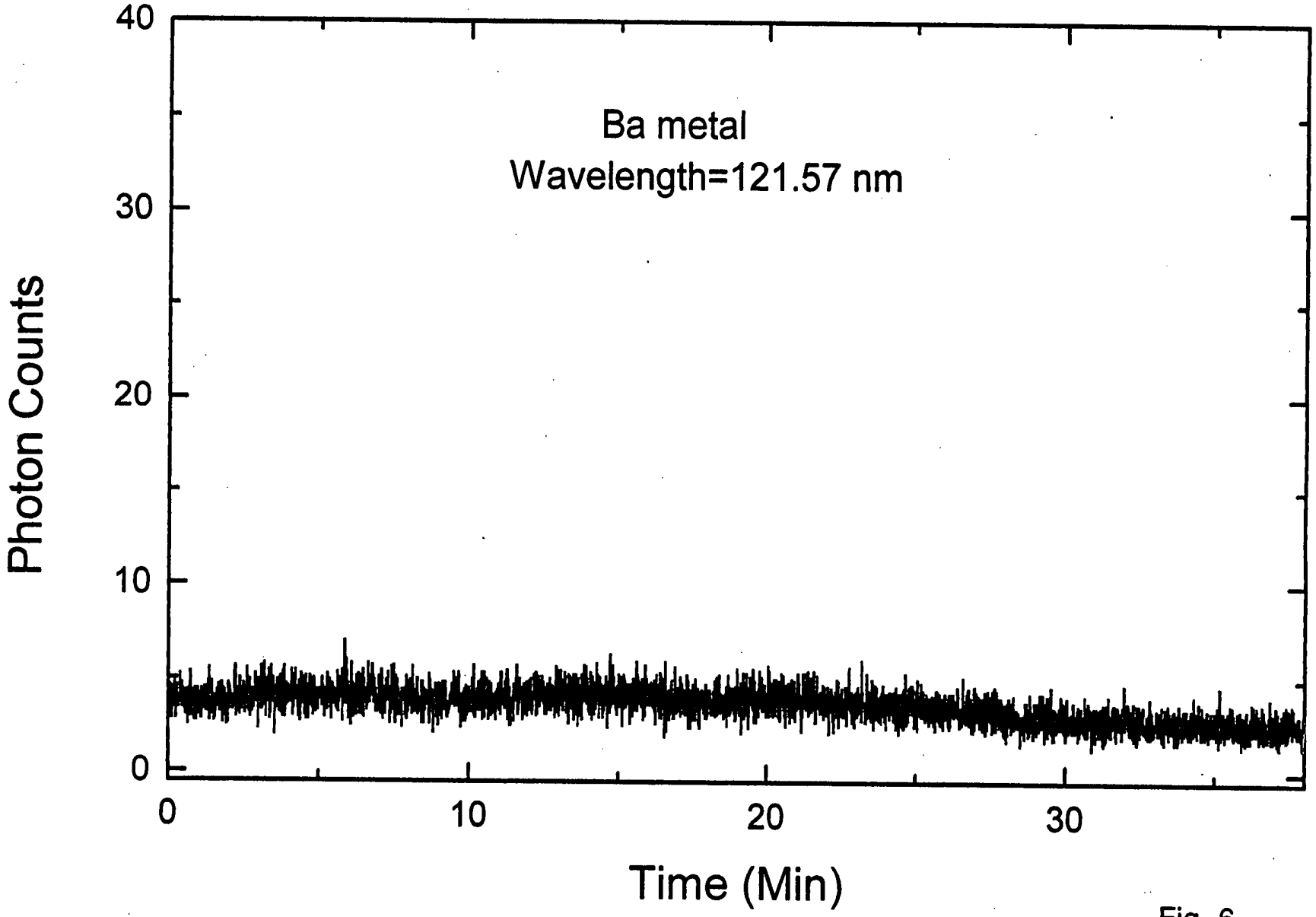
Ba metal
Wavelength=121.57 nm
Photon Counts
Time (Min)
0
10
20
30
40

Fig. 6

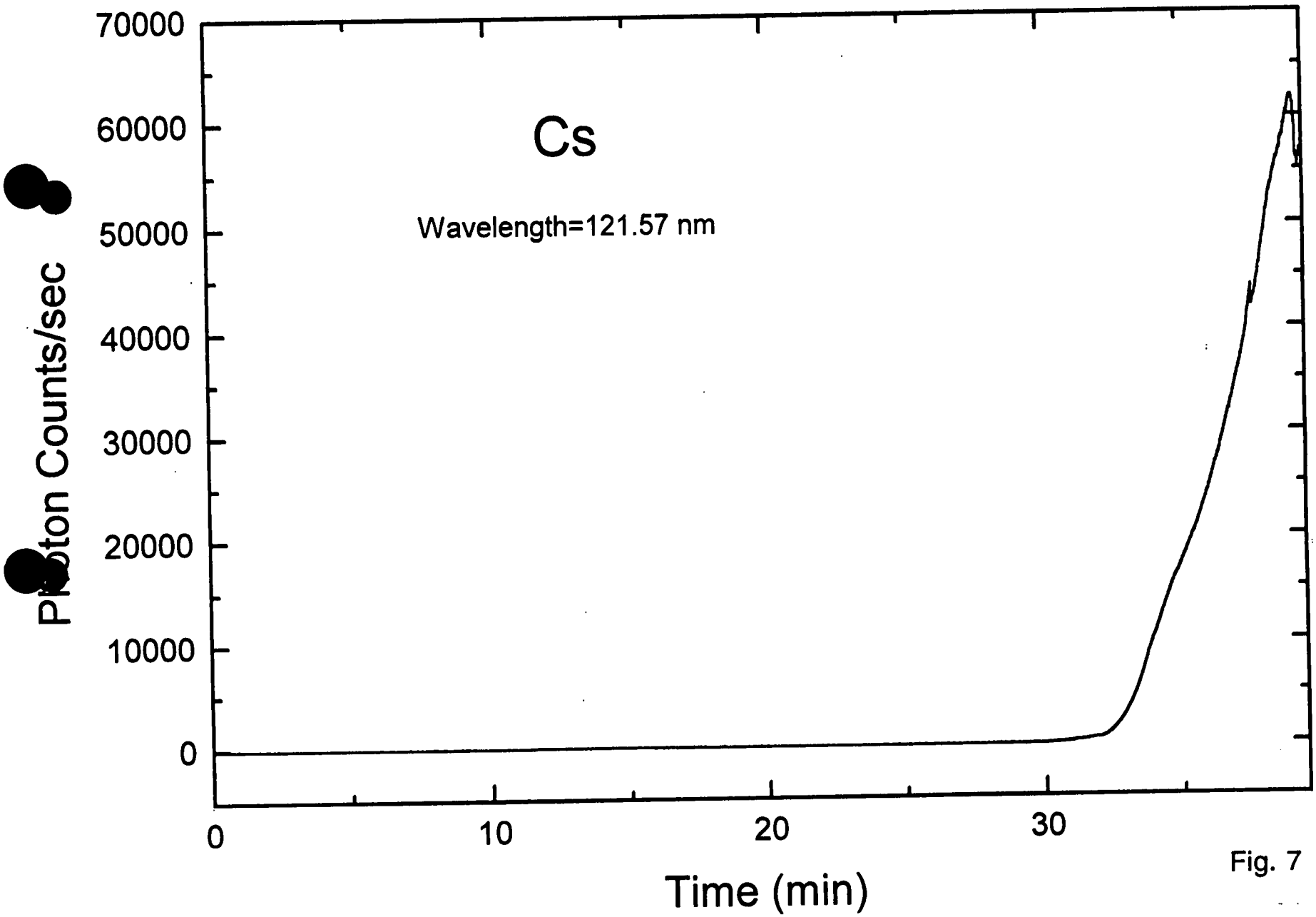
Cs
Wavelength=121.57 nm
Photon Counts/sec
70000
60000
50000
40000
30000
20000
10000
0
0
10
20
30
Time (min)

Fig. 7

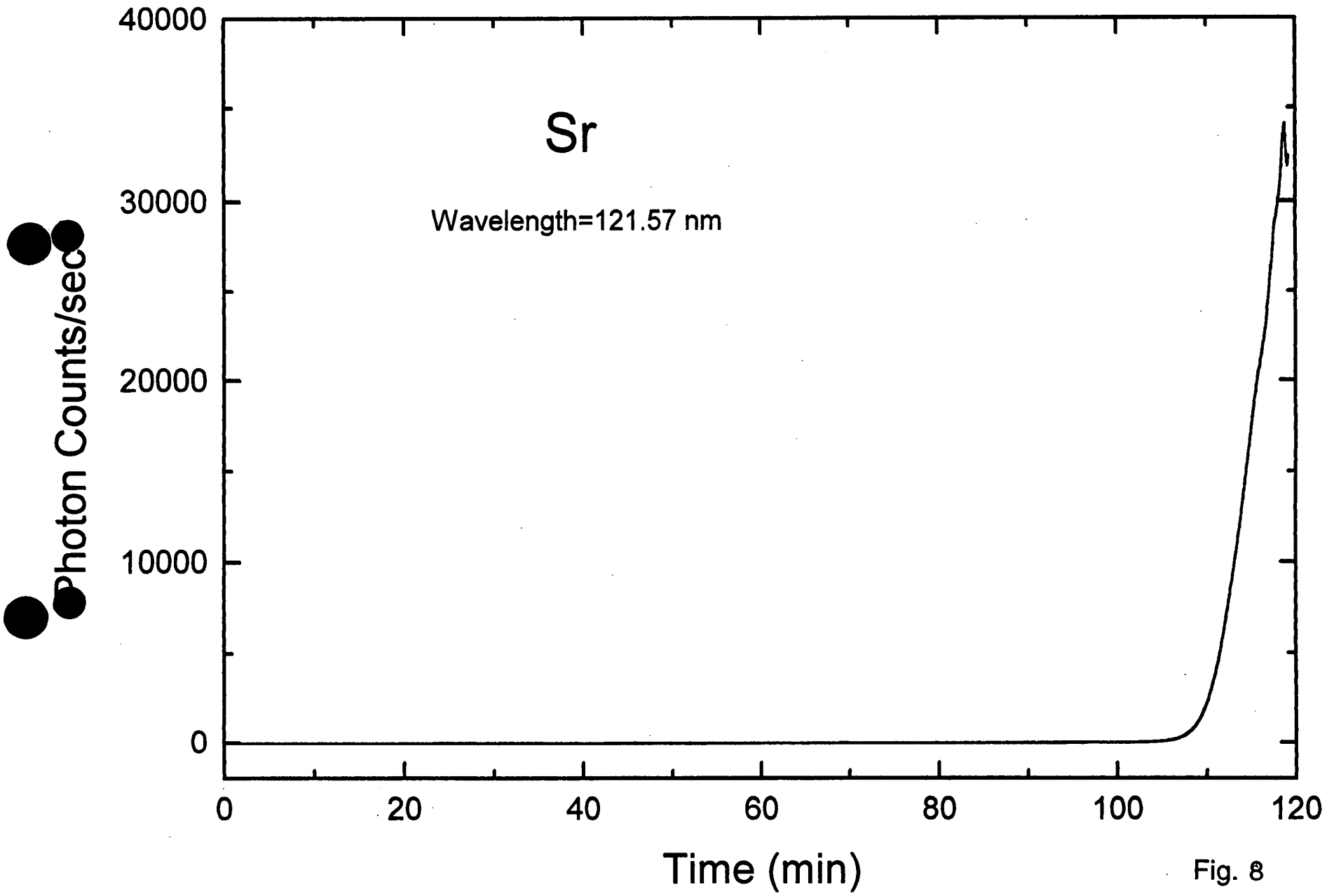
Sr
Wavelength=121.57 nm
Photon Counts/sec
40000
30000
20000
10000
0
0
20
40
60
80
100
120
Time (min)

Fig. 8

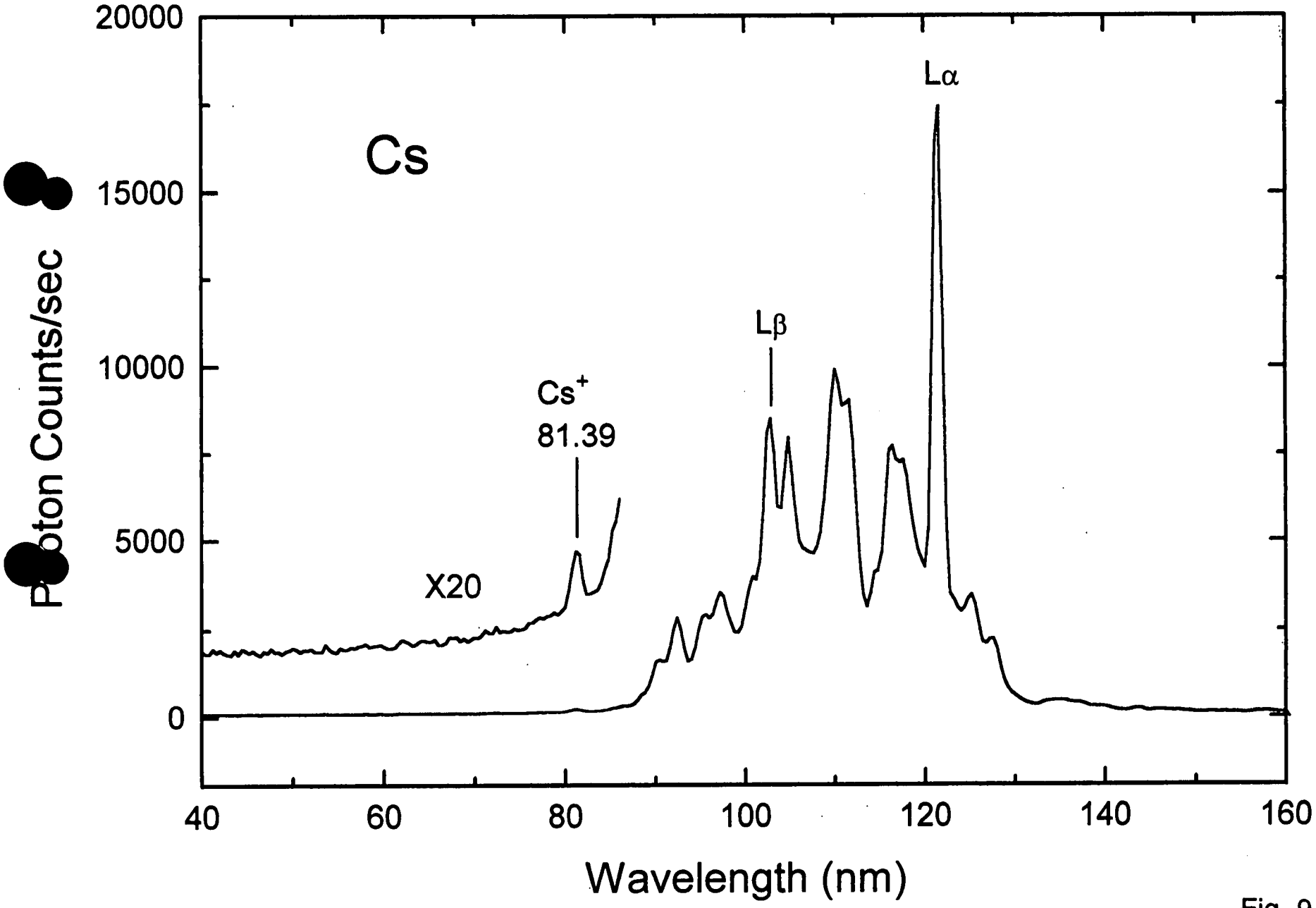
Cs
Lα
Lβ
Cs+
81.39
X20
20000
15000
10000
5000
0
40
60
80
100
120
140
160
Wavelength (nm)

Fig. 9

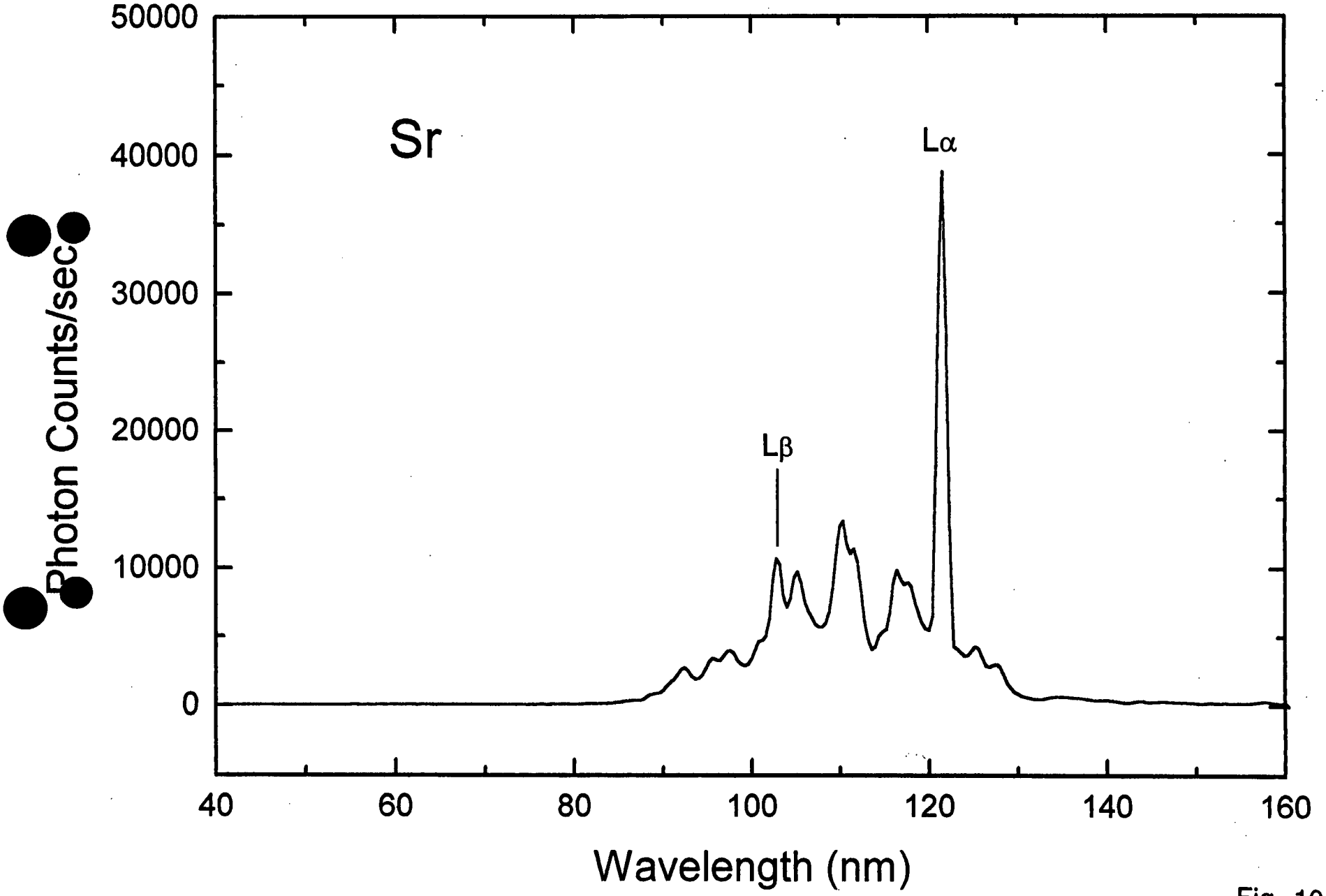
Sr
Lα
Lβ
Photon Counts/sec
50000
40000
30000
20000
10000
0
40
60
80
100
120
140
160
Wavelength (nm)

Fig. 10

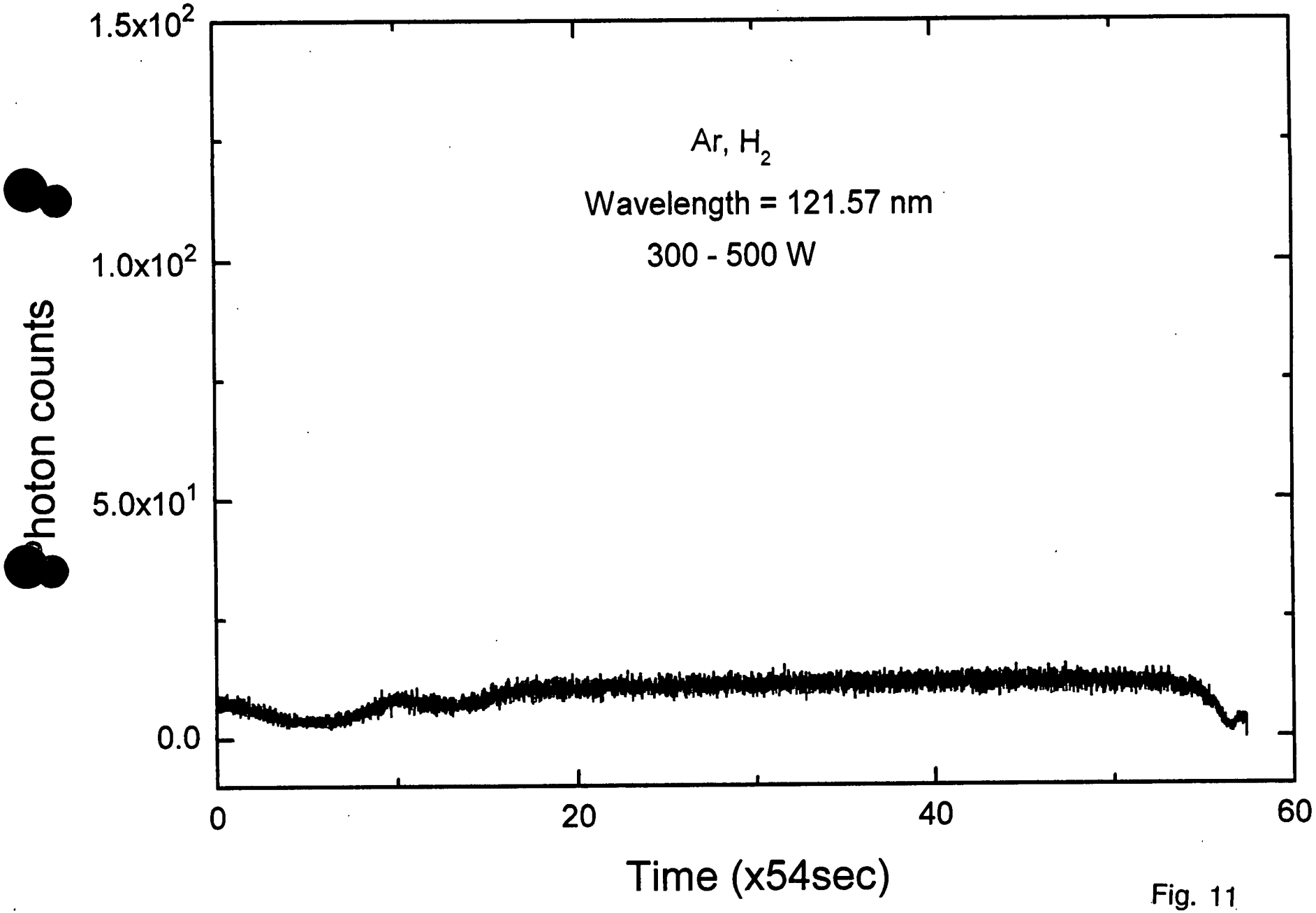
1.5x10^2
1.0x10^2
5.0x10^1
0.0
Photon counts
Ar, H2
Wavelength = 121.57 nm
300 - 500 W
0
20
40
60
Time (x54sec)

Fig. 11

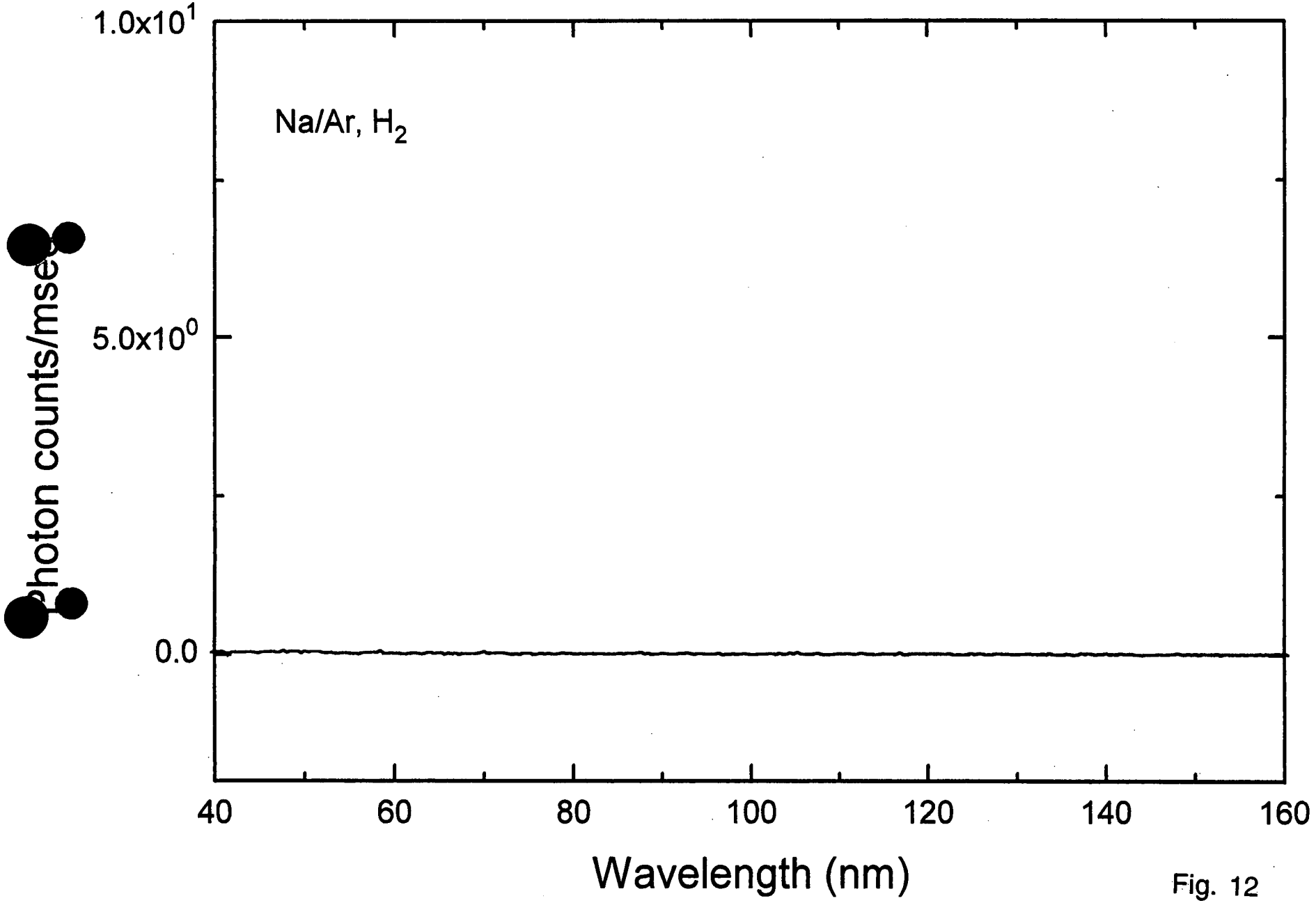
1.0x10^1
Na/Ar, H2
5.0x10^0
0.0
Photon counts/msec
40
60
80
100
120
140
160
Wavelength (nm)

Fig. 12

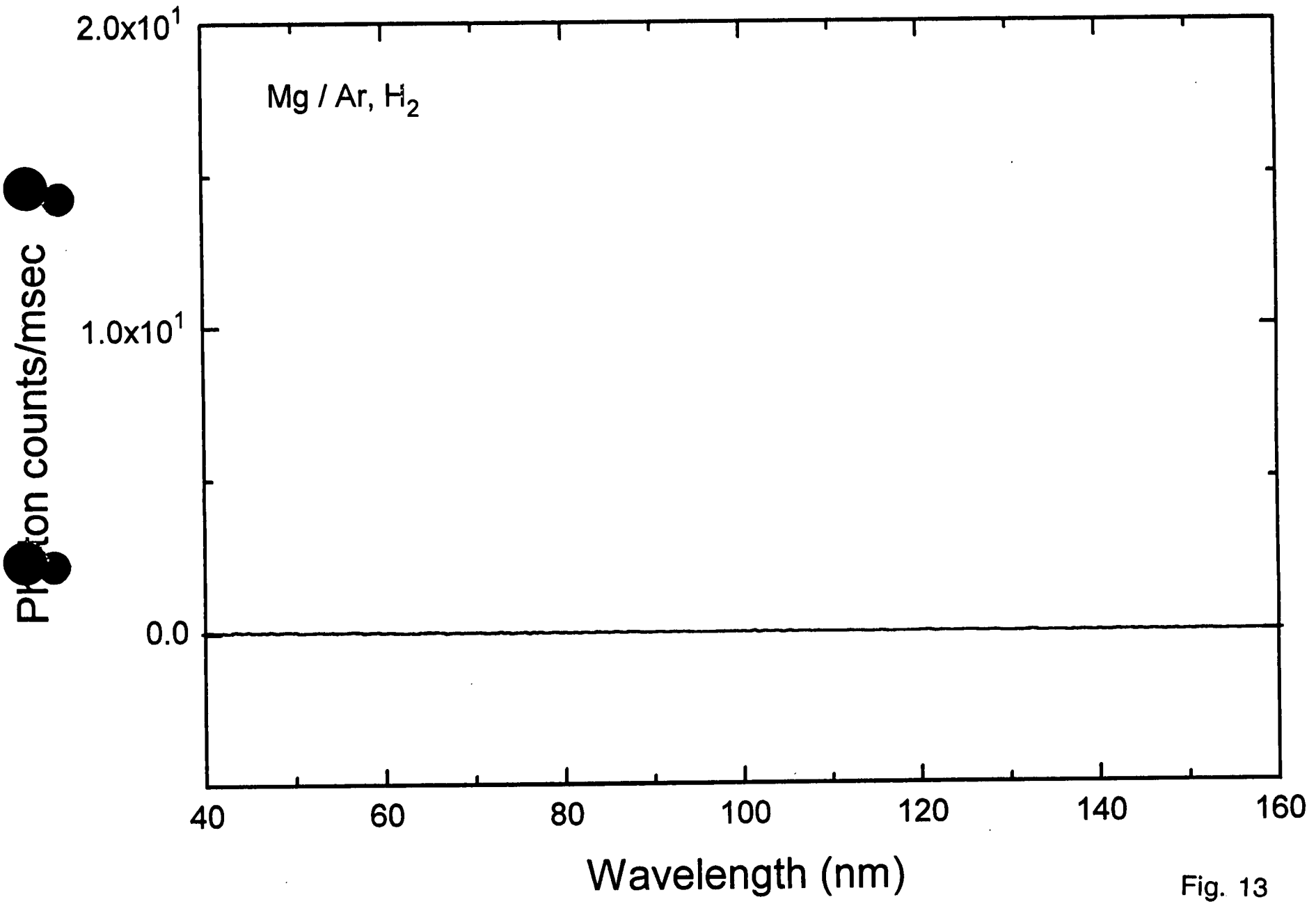
2.0x10^1
Mg / Ar, H2
1.0x10^1
0.0
Photon counts/msec
40
60
80
100
120
140
160
Wavelength (nm)

Fig. 13

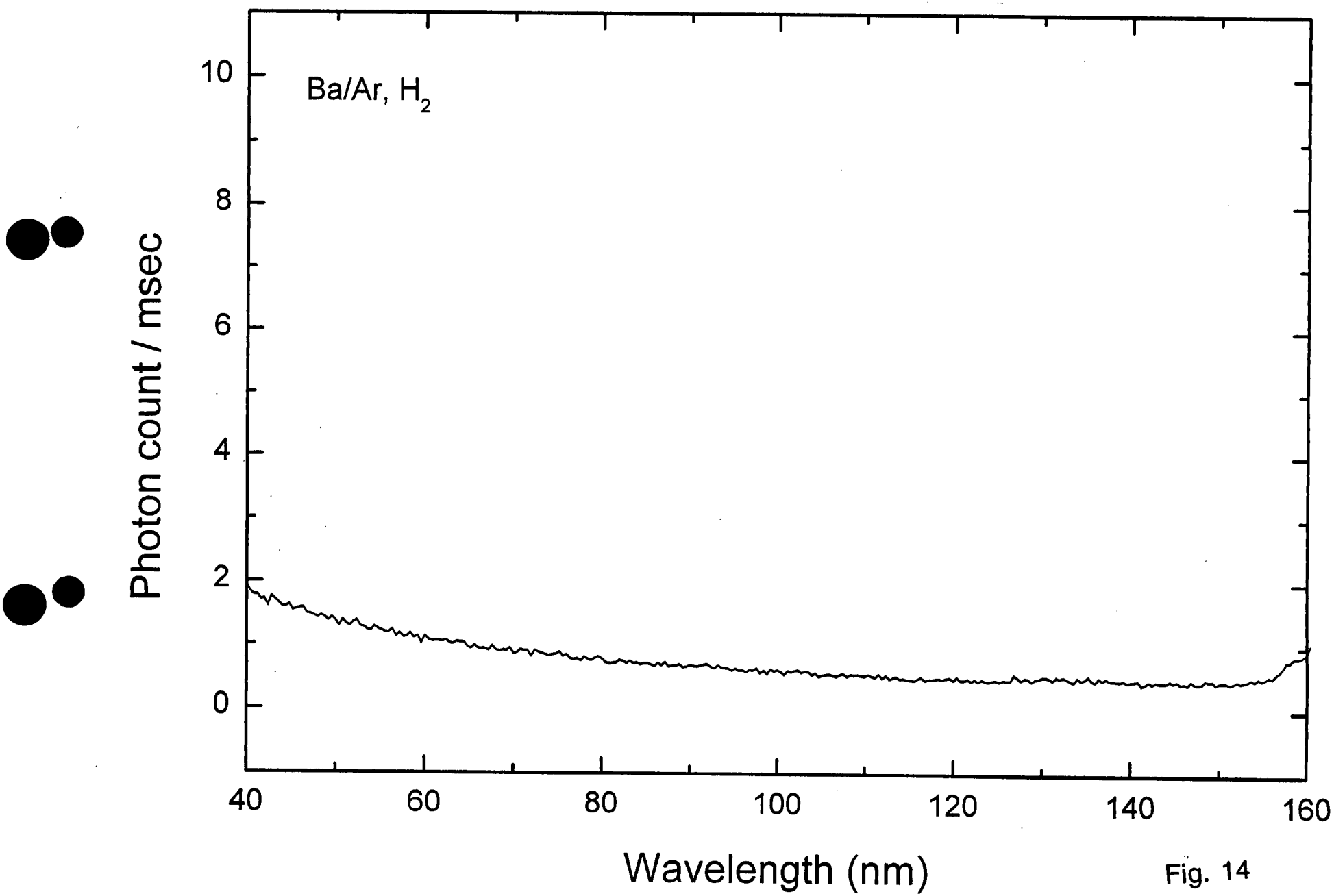
Ba/Ar, H_2
Photon count / msec
Wavelength (nm)
0
2
4
6
8
10
40
60
80
100
120
140
160

Fig. 14